



## Extraction of chitin and chitosan from *Hermetia illucens* breeding waste: A greener approach for industrial application

Samia Elouali<sup>a,b,\*</sup>, Youssef Ait Hamdan<sup>a,c</sup>, Samira Benali<sup>b</sup>, Patrick Lhomme<sup>d,e</sup>,  
Matthias Gosselin<sup>f</sup>, Jean-Marie Raquez<sup>b</sup>, Mohammed Rhazi<sup>a</sup>

<sup>a</sup> Interdisciplinary Laboratory in Bio-Resources, Environment and Materials, Higher Normal School, Cadi Ayyad University, 40000 Marrakech, Morocco

<sup>b</sup> University of Mons (UMONS) - Laboratory of Polymeric and Composite Materials (LPCM), Center of Innovation and Research in Materials and Polymers (CIRMAP), Place du Parc 20, 7000 Mons, Belgium

<sup>c</sup> Univ Rennes, CNRS, ISCR-UMR 6226, F-35000 Rennes, France

<sup>d</sup> Laboratory of Zoology, Research Institute for Bioscience, Mons University, Mons 7000, Belgium

<sup>e</sup> International Centre For Agricultural Research In The Dry Areas, Rabat 10000, Morocco

<sup>f</sup> Laboratory of Entomology, Haute École Provinciale de Hainaut – Condorcet, Ath, Belgium

### ARTICLE INFO

#### Keywords:

Autoclave-assisted process  
Black soldier Fly  
Breeding waste  
Sustainable extraction

### ABSTRACT

Sustainably exploiting the waste of the black soldier fly (BSF) to produce chitin and chitosan remains a challenge. This work valorizes the pupal cases of BSF for chitin and chitosan extraction. Four chemical extraction processes have been employed. Process 1, the standard method for this source, served as a control. Processes 2 and 3 were designed to assess and select the most effective delipidation method, while the optimized Process 4 involved autoclave conditions (121 °C-2.2 Bar). All chitin derivatives obtained were characterized by FTIR, SEM, XRD, <sup>1</sup>H NMR, TGA, potentiometry, viscosimetry, and ICP-OES. Extraction using Process 4 (P4) proved to be the most efficient, demonstrating a deproteinization efficiency of 94.25 ± 0.6 % in a total reaction time of 1.15 ± 0.08 h and water consumption of 250 ± 26.86 L/kg, significantly lower than in other processes. In terms of yield, this process resulted in chitin and chitosan with respective yields of 34.74 ± 1.15 % and 83.33 ± 1.28 %, outperforming the other methods. Regarding physicochemical properties, P4 produced chitin and chitosan with improved thermal stability, with DTG<sub>max</sub> values of 421 °C and 345 °C respectively. Additionally, the crystallinity of chitin was reduced by 25.68 %. For chitosan, the degree of acetylation (DA) was the lowest, while maintaining a high molecular weight of 220,378 g.mol<sup>-1</sup>. These results confirm that P4 is efficient and environmentally friendly, making it well-suited for industrial applications.

### 1. Introduction

Edible insects are emerging as promising sources of biomass, due to their distinctive composition [1] – i.e., they are rich in proteins [2], fats [3] and biopolymers. Their ability to thrive on biological waste streams, coupled with their substantial dry matter content, establishes them as optimal biosources for chitin and chitosan production [4]. Moreover, they serve as a quintessential model within the framework of the circular bioeconomy, enabling the efficient conversion of waste into high-value outputs such as biodiesel, enhanced energy recovery, reduced greenhouse gas emissions [5,6] and bioactive materials like chitin and chitosan. Chitin, among the most prevalent polysaccharides globally,

exhibits broad utility upon conversion into chitosan through partial N-deacetylation under alkaline conditions [7]. Renowned for its renewable, biodegradable, and non-toxic nature, chitosan possesses various properties, including filmogenic, biological, and antifungal activities [8,9]. The chitin and chitosan industry, owing to its versatile applications across various sectors such as cosmetics [10], bioplastic production [11], water treatment [12] and other industries [13–20], is expanding rapidly and represents a steadily growing global market. Estimations place its market size at USD 1.75 billion in 2023 and USD 1.96 billion in 2024 [21], with the primary source of commercialized chitin and chitosan derived from waste streams of the marine food industry [22], notably from shrimp shells and crabs (Table 1). Projections suggest a

\* Corresponding author at: Interdisciplinary Laboratory in Bio-Resources, Environment and Materials, Higher Normal School, Cadi Ayyad University, 40000 Marrakech, Morocco; University of Mons (UMONS)-Laboratory of Polymeric and Composite Materials (LPCM), Center of Innovation and Research in Materials and Polymers (CIRMAP), Place du Parc 20, 7000, Mons, Belgium.

E-mail address: [samia.ELOUALI@umons.ac.be](mailto:samia.ELOUALI@umons.ac.be) (S. Elouali).

<https://doi.org/10.1016/j.ijbiomac.2024.138302>

Received 3 June 2024; Received in revised form 20 November 2024; Accepted 1 December 2024

Available online 3 December 2024

0141-8130/© 2024 Elsevier B.V. All rights reserved, including those for text and data mining, AI training, and similar technologies.

**Table 1**  
Advantages and disadvantages of each chitin source.

Source	Advantages	Disadvantages	Ref
Crustaceans (Shrimp, Crab, Lobster)	<ul style="list-style-type: none"> <li>- Well-established extraction methods with high efficiency</li> <li>- High chitin content (up to 30 % of dry weight)</li> <li>- Commercially available and widely used in various industries</li> <li>- Good mechanical properties of extracted chitin, making it suitable for diverse applications</li> </ul>	<ul style="list-style-type: none"> <li>- Seasonal availability can limit supply</li> <li>- Potential allergens (e.g., tropomyosin) that may pose health risks</li> <li>- Requires harsh chemical treatments (HCl) due to the high mineral content that may damage chitin structure and lead to environmental pollution</li> </ul>	[7,22,24]
Insects (e.g., BSF puparia)	<ul style="list-style-type: none"> <li>- Year-round availability, allowing for consistent supply</li> <li>- Higher chitin content in some species (up to 40 % of dry weight)</li> <li>- More sustainable and eco-friendly, with lower carbon footprint</li> <li>- Potential for higher yields and simpler extraction processes compared to crustaceans</li> </ul>	<ul style="list-style-type: none"> <li>- Less established extraction methods compared to crustaceans, requiring further optimization</li> <li>- Variability in chitin quality depending on species and extraction method</li> <li>- Limited commercial availability and market acceptance, affecting scalability</li> </ul>	[25–27]
Fungi (e.g., Termitomyces, Ganoderma)	<ul style="list-style-type: none"> <li>- Renewable and sustainable source with minimal environmental impact</li> <li>- Absence of allergenic proteins, making it safer for consumption</li> <li>- More environmentally friendly with lower disposal costs and potential for waste substrate utilization</li> </ul>	<ul style="list-style-type: none"> <li>- Lower chitin content compared to crustaceans and insects (typically around 5–10 % of dry weight)</li> <li>- Extraction methods still being optimized, with less standardization</li> <li>- Potential risks of pathogenic fungi if not handled properly</li> </ul>	[25]
Squid Pens	<ul style="list-style-type: none"> <li>- Renewable source with minimal environmental impact and year-round</li> <li>- Can be processed with fewer environmental concerns compared to crustaceans</li> </ul>	<ul style="list-style-type: none"> <li>- Lower chitin content compared to crustaceans (typically around 15–20 %)</li> <li>- Limited commercial use and availability, affecting market viability</li> <li>- Extraction methods may not be as well-developed as those for crustaceans</li> </ul>	[28]

robust growth trajectory, with the market expected to reach USD 4.07 billion by 2030, propelled by a compound annual growth rate (CAGR) of 12.80 %. However, impediments to this growth abound, primarily linked to challenges surrounding the main chitin resources. Seasonal fluctuations in the availability of marine food waste [22], supply chain shortages, and ecological degradation stand as prominent obstacles [23]. Addressing these challenges necessitates the identification of more economically viable alternative sources of chitin. Table 1 presents the advantages and disadvantages of various natural sources used to isolate chitin.

The Black Soldier Fly (BSF), *Hermetia illucens*, is one of the edible insects that play a pivotal role in organic waste recycling, effectively converting waste nutrients into valuable resources and reducing waste volume. The BSF larvae have also been used to recycle meat and bone meal [6], and to convert protein-rich waste into biodiesel [5]. It is recognized for its abundant proteins, lipids, minerals, and chitin content

[29], being considered a key species in this regard. Additionally, BSF reproduce rapidly under suitable environmental conditions and could serve as alternative sources to produce chitin and chitosan [30]. Several research studies have been focused on obtaining chitin from its various stages, particularly the puparial cases, known as the third chitin-rich byproduct in the life cycle of the BSF. However, due to its richness in proteins, lipids, and minerals, the pupal stage of *Hermetia illucens* requires more stringent conditions for the isolation of chitin, its purification, bleaching to eliminate impurities and pigments that resist extraction [10,31,32]. To achieve this, more chemicals are consumed, including additional acids and bases for demineralization and deproteinization due to the increased number of repeated baths and steps required for chitin and chitosan purification. Consequently, the reaction will systematically last longer, and reflux heating during the reaction with the washings sample will consume more water and energy, which contradicts Sustainable Development Goals (SDGs) 6 and 12, which aim to ensure sustainable management of water resources and promote sustainable consumption – i.e., water, chemical products and energy. Additionally, all these severe conditions will impact the quality and yield of both chitin and chitosan. Indeed, the major problem encountered in chitin chemistry lies on its preparation and extraction to obtain chitin with characteristics close to its native form in terms of molar mass, acetylation degree and crystalline properties.

To address the need for sustainable scalability in chitin and chitosan production, this study explores alternative, rapid and eco-friendly extraction methods aimed at industrial feasibility. This approach was based on autoclave-assisted extraction, which has been adopted for the deproteinization step, resulting in a significant reduction in extraction duration compared to conventional methods [33] and for the sterilization of the raw material after the demineralization step by Lagat et al. [34] maintaining the high quality of chitin.

This work aims to elucidate the impact of each extraction step, specifically examining BSF puparial cases as a chitin source without any additional nutritional modification. To the best of knowledge, this method has not been previously applied to extract chitin from BSF puparial cases or to produce chitosan under the specific conditions tested (121 °C, 2.2 bar) using a mixture of 50 % KOH, 25 % ethanol, and 25 % mono-ethylene glycol. Various chitin extraction methods were evaluated, with particular attention to delipidation, a step often overlooked but shown here to significantly impact the purity of both chitin and chitosan. Four distinct extraction processes were compared: the standard chemical method without delipidation (P1), methods incorporating delipidation through Hexane solvent (P2) and Methanol-chloroform mixture (P3) and a fourth process (P4) that applied the autoclave-assisted technique for deproteinization and deacetylation. This work identifies an optimal, scalable extraction protocol that minimizes chemical and water consumption, reduces processing time, and improves the physicochemical properties of the final chitosan product.

## 2. Material and methods

### 2.1. Insect material

The BSF samples used in this study were supplied by the company EntomoNutris located in Marrakech (Morocco). The larvae were reared from hatching until pupation on chick feed (Alf Sahel S.A) at 70 % water content, within plastic containers (37 × 31 × 10 cm), with a density of 8.7 larvae/cm<sup>2</sup> (10,000 larvae/crate). The larvae were raised in climate-controlled conditions at 28 °C and 60 % relative humidity. Upon adult emergence, puparial cases of BSF were harvested, dried at 50 °C for 24 h, and then finely ground using a Retsch RM 200 mortar grinder to obtain particle sizes between 0.4 mm and 0.6 mm.

## 2.2. Composition of the insect material

### 2.2.1. Ash content

Ash content was determined by incinerating samples at 550 °C at a constant rate of 50 °C every 30 min for 4 h, followed by cooling in a desiccator [35]. The ash content was calculated using the following Eq. (1):

$$\text{Ash (\%)} = \frac{W_2 - W_0}{W_1 - W_0} \times 100 \quad (1)$$

where  $W_0$  is the constant weight of crucible,  $W_1$  is the weight of the sample and crucible and  $W_2$  is the weight of the ash and the crucible.

### 2.2.2. Water content

The water content was determined by dehydrating samples at 110 °C for 24 h. It was calculated based on the following Eq. (2):

$$\text{Water (\%)} = \frac{m_{ds}}{m_{rm}} \times 100 \quad (2)$$

where  $m_{ds}$  is the weight of dehydrated samples and  $m_{rm}$  is the weight of the raw material.

### 2.2.3. Lipid content

Lipid content was analyzed by a rotavapor (Heidolph) at 60 °C for 20 min after the defatting step [36]. The delipidation bath was then placed under the rotavapor to remove the solvent; the remaining residue corresponded to the eliminated lipids. Lipid (%) content was calculated by weighing.

### 2.2.4. Protein content

Kjeldahl method has been employed following the procedure described by Liu et al. [37], to determine the protein content in the BSF samples. 1 g of the sample was subjected to catalytic heating to break down the proteins present in the raw material. Subsequently, 0.5 M of sulfuric acid was added to convert the released ammonia into ammonium sulfate. Alkaline distillation was employed to separate the free ammonia, which was then absorbed by boric acid and titrated with hydrochloric acid (0.1 M). The results are reported as a percentage.

### 2.2.5. Mineral content

Inductively Coupled Plasma Optical Emission Spectroscopy (ICP-OES), using the iCAP 7000 instrument from ThermoFisher Scientific, with a high sensitivity of <1 ppm, was utilized for the quantitative and qualitative determination of mineral content.

## 2.3. Quantification of water consumption

An iPERL water meter from SENSUS is used to count the quantity of water during each extraction process and the water used for washing. The meter has a DN15–3/4" (20x27mm) size - L.110 mm - 2.5m<sup>3</sup>/h capacity.

## 2.4. Chitin extraction

To extract chitins, four processes with several steps were adopted in this study (Table 2). For delipidation, the Soxhlet extraction method using hexane solvent [38] and Folch method using Methanol-chloroform mixture 1:4 (v/v) as a solvent were selected. Demineralization was carried out using an HCl solution (0.55 M) with a ratio of 1:10 (w/v) at room temperature for 1 h. The deproteinization step involved an alkaline treatment using repeated baths of NaOH solution (1 M) at a ratio of 1:10 and maintained at 80 °C under reflux heating and a 1 M NaOH solution within an autoclave at 121 °C for 15 min at a ratio of 1:20 (w/v). In parallel, deproteinization was carried out concurrently with the quantification of proteins removed at 595 nm using the Bradford method

**Table 2**

Chitin extraction by processes P1, P2, P3 and P4.

Processes	Delipidation	Demineralization	Deproteinization
P1	–	0.55 M HCl / 25 °C 1 h / 1:10 (w/v)	1 M NaOH / 80 °C 18 h / 1:20 (w/v)
P2	Hexane / 60 °C 1 h / 1:20 (w/v)	0.55 M HCl / 25 °C 1 h / 1:10 (w/v)	1 M NaOH / 80 °C 18 h / 1:20 (w/v)
P3	Methanol-chloroform / 25 °C 1 h / 1:20 (w/v)	0.55 M HCl / 25 °C 1 h / 1:10 (w/v)	1 M NaOH / 80 °C 18 h / 1:20 (w/v)
P4	Methanol-chloroform / 25 °C 1 h / 1:20 (w/v)	0.55 M HCl / 25 °C 1 h / 1:10 (w/v)	1 M NaOH / 121 °C-2.2 Bar 1 h15 / 1:20 (w/v)

[39], a volume of 20 µL of each deproteinization bath is mixed with 3 mL of Bradford solution (Coomassie Blue G-250, ethanol and water). All obtained chitins were washed until pH neutral and dried at 40 °C for 24 h. The chitins yield (%) was determined using the following Eq. (3):

$$\text{Chitin (\%)} = \frac{m_{chitin}}{m_{raw\ material}} \times 100 \quad (3)$$

Where  $m_{chitin}$  represents the weight of chitin obtained after demineralization, delipidation and deproteinization steps,  $m_{raw\ material}$  represents the weight of the insect material.

## 2.5. Chitosan preparation

Chitosans were prepared using two processes. A mixture of 50 % potassium hydroxide (KOH), 25 % ethanol and 25 % mono-ethylene glycol with a ratio of 1:60 (w/v) was used at 120 °C for 24 h under agitation. The same mixture was used under autoclave conditions (121 °C – 2.2 bar) for 1 h with a ratio of 1:10 (w/v), which provided <6 times the quantity of chemical products for the deacetylation step. Four chitosan samples were washed with distillate water until neutrality and dried at 40 °C for 24 h. The chitosan yield (%) was determined using the following Eq. (4):

$$\text{Chitosan (\%)} = \frac{m_{chitosan}}{m_{chitin}} \times 100 \quad (4)$$

where  $m_{chitosan}$  represents the weight of chitosan obtained after deacetylation,  $m_{chitin}$  represents the weight of the chitin.

## 2.6. Physicochemical characterization

### 2.6.1. FTIR characterization

FTIR spectra were performed on Jasco 4600 A Gemini FT-IR sampling spectrometer. The spectra allowed for the determination of the characteristic area of the acetylated amine function around 1655 cm<sup>-1</sup>, and the reference peak of the amine function around 3450 cm<sup>-1</sup>. Subsequently, the degree of acetylation (DA) was calculated using the following formula (5) [40].

$$\text{DA (\%)} = \frac{A_{1655}}{A_{3450}} \times 115 \quad (5)$$

### 2.6.2. SEM-EDX

Samples were analyzed in VEGA3 TESCAN device. The morphology of the prepared chitins (CHT P1, P2, P3 and P4) and chitosans (CHS P1, P2, P3 and P4) was observed by magnification at 50 µm.

### 2.6.3. Molecular weight determination

The Ubbelohde capillary viscometer (0.5–3 mm<sup>2</sup>/s, 15–20 mL) was used to determine the viscometric molar mass of chitosan at 25 °C. The solution used is a mixture of 0.3 M acetic acid and 0.2 M sodium acetate [41]. The average molecular weight viscosity was calculated from the following Mark Houwink Eq. (6) [42].

$$[\eta] = K \cdot M^a \quad (6)$$

With  $[\eta]$  is the intrinsic viscosity,  $M$  is the viscometric molar mass.  $K$  and  $a$  are the viscometric constants determined in the literature [43].

#### 2.6.4. X-ray diffraction XRD analysis

The device used for recording the results is a Rigaku III diffractometer (Rigaku Corp, Japan) with Cu radiation (40 kV, 30 mA). Data were collected with a scan angle of  $5^\circ$  to  $40^\circ$ . The crystallinity index ( $I_{Cr}$ ) is determined using the following [44].

$$I_{Cr}(\%) = \frac{S_c}{S_t} \times 100 \quad (7)$$

where  $S_c$  is the area of the crystal domain and  $S_t$  is the area of the total domain.

#### 2.6.5. Potentiometry titration

Chitosan was solubilized in a 0.1 M HCl solution and then neutralized with a 0.1 M NaOH solution. The titration curve showed two inflection points: the first corresponding to excess acid and the second to the neutralization of protonated chitosan [45]. The acetylation degree (DA) was calculated according to the Eq. (8) [46].

$$DA(\%) = 1 - \frac{16,1(x_2 - x_1)}{m - m'} \times N \quad (8)$$

where  $N$  is the molarity of NaOH solution,  $m$  is the mass in grams of chitosan and  $m'$  is the mass of water content in a sample.

#### 2.6.6. $^1H$ NMR characterization

$^1H$  NMR was carried out on a 400 MHz Bruker, using  $D_2O/DCI$  (2%) to solubilize 20 mg of chitosan. The solution was heated at  $70^\circ C$  for 1 h to accelerate the dissolution. NMR chemical shifts are reported in ppm [47].

The integrals of the H-1-D peak and the integrals of the H-Acetyl peak serve as a basis to calculate the DA of chitosan following the Eq. (9) [40].

$$DA(\%) = 1 - \frac{(H - 1 - D)}{(H - 1 - D + 1/3 HAC)} \times 100 \quad (9)$$

#### 2.6.7. Thermal analysis

Thermogravimetry (TGA) measurements were performed using a TGA Q500 instrument under  $N_2$  gas atmosphere at 0.1 MPa. The chitins and chitosans were heated from  $20$  to  $600^\circ C$  with a heating rate of  $20^\circ C \cdot min^{-1}$ .

#### 2.6.8. Statistical analysis

Statistical analysis of the data was carried out using GraphPad Prism version 9.00 software (San Diego, California, USA). Results are presented as mean  $\pm$  SEM. An analysis of variance (ANOVA) was performed, followed by Tukey post-hoc tests with a significance level of  $p = 0.05$ .

### 3. Results and discussion

#### 3.1. Chitin and chitosan production

Before any extraction process, it is essential to characterize the composition of the raw material, the steps of chitin and chitosan extraction are presented in Fig. 1 according to the chemical composition of the insect material.

The analyses of BSF (pupal cases) show that they are composed of  $7.80 \pm 0.02\%$  of water,  $16 \pm 0.01\%$  of ash and  $5.50 \pm 0.01\%$  of lipid (Table 3). Compared with the literature, the lipid content determined is close to that cited by Triunfo et al. [48], which is around 5%. Regarding this lipid content concerning the other stages of the BSF, the content of lipids remains lower than in other stages due to the transformation of lipids into an energy source during metamorphosis in the life cycle of these insects [37,49].

**Table 3**  
Chemical composition of BSF puparial cases.

	Lipid	Mineral	Protein	Water	Ash content	Other
Weight (%)	$5.50 \pm 0.01$	$4.34 \pm 0.03$	$42.60 \pm 0.02$	$7.80 \pm 0.02$	$16 \pm 0.01$	$23.66 \pm 0.03$

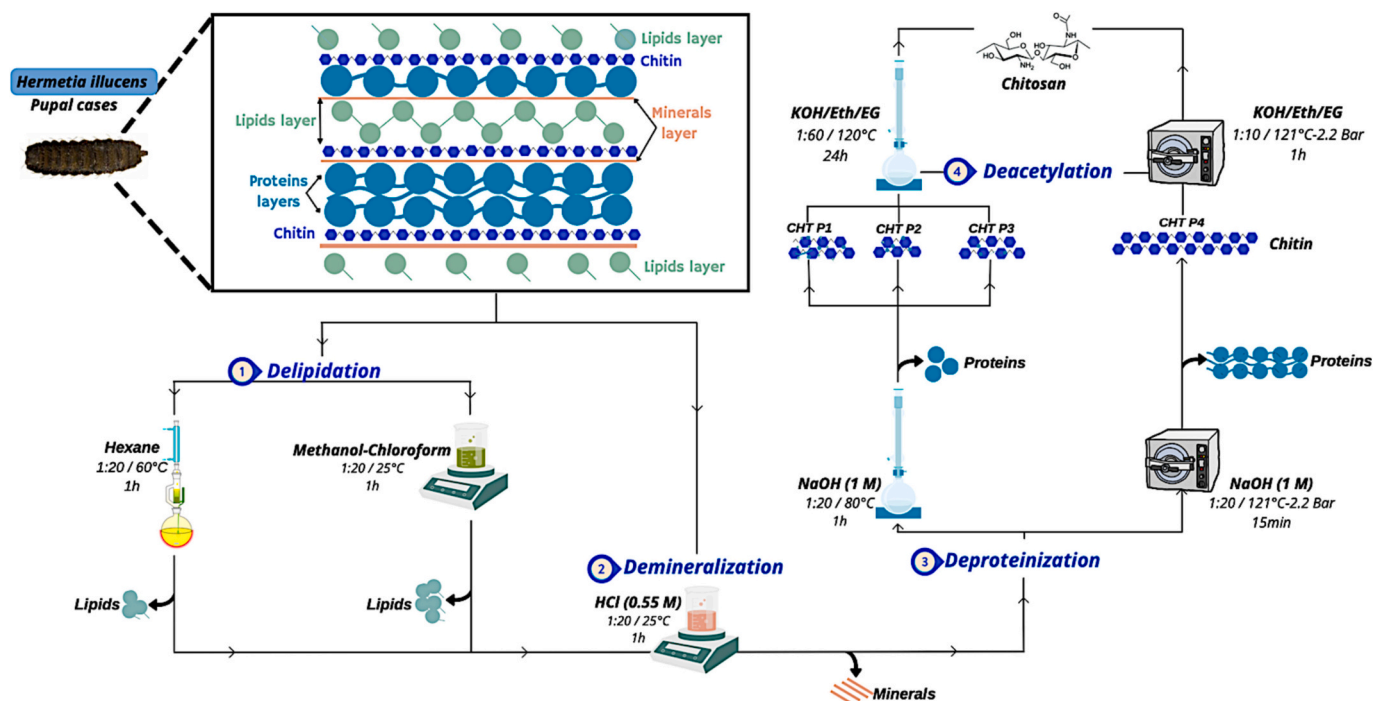


**Fig. 1.** Steps for chitin extraction and chitosan elaboration from BSF (pupal cases).

The pupal stage of BSF contains a total mineral content of  $4.34 \pm 0.03$  % predominantly comprised of 1.37 % K, 0.92 % Cl and 0.78 % Na. Additionally, tiny amounts of other elements such as Mg, Ca, Al and P were detected at lower percentages varying from 0.19 to 0.49 % (Table 4). Generally, empty puparia of BSF is known for its low mineral content compared to other stages of BSF and other insects fed [37], which is confirmed by the absence of effervescence during the demineralization step. The lowest concentration of hydrochloric acid was used compared to the literature [50] reducing acid consumption by 75 % in this step.

The protein content composed the insect material is around 42.60 %, this value is correlated with that determined in *Hermetia illucens* larvae by Nafisah et al., with a content of 42.99 % [51], and by Liland et al., which is around 40 % [52]. This data shows us the diversity of compounds contained in BSF puparial cases and confirms the significance of this study and the need to proceed with the elimination of lipids, minerals and even proteins and total impurities.

The kinetics of deproteinization were evaluated using four extraction processes (P1, P2, P3 and P4). The protein content for each extraction bath was quantified using the Bradford method, allowing the construction of individual curves for each method and a comparison of their efficiency and rate (Fig. 2). These observations revealed a progressive increase in the quantity of eliminated proteins across all four extraction processes compared to the respective baths. However, the deproteinization rate varies depending on the extraction process used.

Even though the researcher relied on the disappearance of the bath coloration as evidence of deproteinization [53], the kinetics studied by Bradford assay at 595 nm do not confirm it in this case. The baths were found to be colorless for processes P1, P2, P3, and P4 respectively at the 9th, 8th, 6th and 3rd baths. This confirms that the pupal stage of BSF remains rich in proteins [37], whether responsible or not for the pigmentation of this species. After deproteinizing up to the 5th bath by process P4, the obtained chitin is clear and whitish in appearance (Fig. 3). This was deemed unnecessary for whitening purposes. Notably, the autoclave process P4, emerged as the most proficient, successfully eliminating  $94.25 \pm 3.79$  % of protein in just 5 baths for 75 min (15 min/bath) (Fig. 4). This method stands out as the most efficient process for rapid and economical deproteinization.

Based on the use of the flowmeter during the deproteinization step, a flow rate of 23 mL/min is used for reflux heating during this reaction to ensure the conservation of the solution used. A volume of 100 mL of distilled water is used to prepare the 1 M NaOH solution for 5 g of raw material, and 3 L is also used for washing the deproteinized material after each bath. Projecting this onto the number of baths, which is systematically linked to the variation in water consumption during reflux, reaction, and washing, nearly 80 L of distilled water is consumed to deproteinize 5 g of *H. illucens* empty puparia with a low deproteinization efficiency of <40 % by the usual process P1. However, an 80 % reduction in water consumption is achieved by using process P4 – i.e. around 15 L vs 80 L for P1 - with a deproteinization efficiency >94 %. Projected onto a normalization of water consumed for the production of 1 kg of chitin across the four processes (Fig. 4), >1300 l of water are saved by P4 (instead of P1).

Following the protein analysis, process P4 exhibited the highest protein removal efficiency. Therefore, the elimination of proteins across the various processes can be ranked in the following order, where QPE is the quantity of proteins eliminated by each process:

$$QPE (P4) > QPE (P3) > QPE (P2) > QPE (P1).$$

From a performance standpoint, a significant difference is observed

**Table 4**  
Mineral content of BSF pupae.

Minerals	K	Cl	Na	Mg	Ca	Al	P
(%)	1.32	0.92	0.78	0.49	0.30	0.29	0.19
	$\pm 0.01$	$\pm 0.01$	$\pm 0.00$	$\pm 0.02$	$\pm 0.02$	$\pm 0.01$	$\pm 0.00$

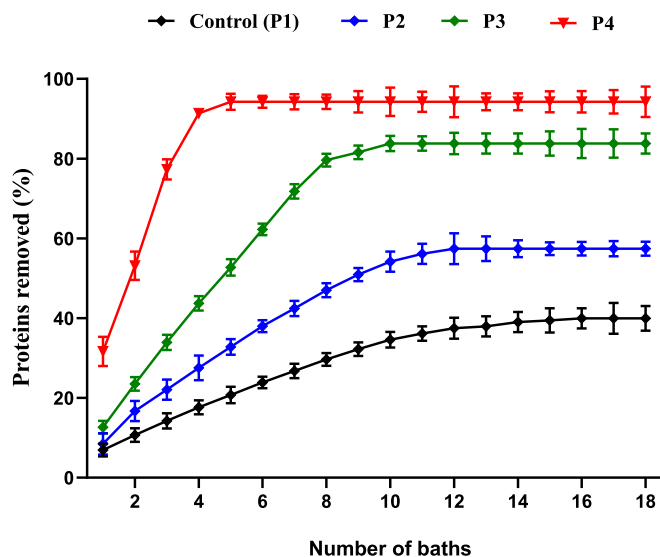


**Fig. 2.** Kinetic of deproteinization step by processes P1, P2, P3 and P4.

between the two lipid removal methods adopted in the extraction processes. This could be attributed to the heating involved in the Soxhlet protocol, which may degrade the material during delipidation. Considering this variance, a methanol-chloroform mixture in a 1:4 ratio was chosen for processes P3 and P4 to maintain a higher yield of 97.27 %. Due to the low mineral content in the insect material, only one bath is utilized for this step. However, in terms of deproteinization, there is a considerable discrepancy in yield ranging from 19 % to 41 %.

Regarding the chitin yields obtained by the four processes (Table 5), P4 shows the highest yield at  $34.74 \pm 1.15$  %. This yield is higher than the chitin yields reported in several studies on the extraction of chitin from BSF using chemical and biological methods [29,34,54,55]. However, chitosan yields (related to chitin) obtained vary from  $68.57 \pm 1.15$  to  $83.33 \pm 1.15$ . This range is similar to the yield of chitosan prepared from *Tenebrio molitor* beetles, which typically falls between 76.43 % and 78.26 % [56].

### 3.2. Physicochemical properties

The XRD analysis of chitins (CHT P1, P2, P3 and P4) (Fig. 5(a)) shows two peaks around  $9^\circ$  and  $19^\circ$ , corresponding to (020) and (110) reflection planes respectively [57]. Additionally, three low-intensity peaks were observed at  $13^\circ$ ,  $23^\circ$  and  $26^\circ$ , corresponding to (021), (101) and (130) planes. These peaks exhibit the characteristic alpha chitin form [58]. Moreover, in CHT P1, a peak at  $28^\circ$  is observed, which could indicate interactions with mineral components present in this source that persist even after the demineralization step [59]. Following the deacetylation of chitins, the results of chitosan (CHS P1, P2, P3, and P4) show the disappearance of peaks around  $9^\circ$ ,  $13^\circ$ ,  $19^\circ$ ,  $23^\circ$ , and  $26^\circ$  (Fig. 5(b)), with the appearance of two new peaks at around  $10^\circ$  and  $20^\circ$ , which are characteristic of chitosan [60]. The peaks became less intense after deacetylation, indicating a difference in crystallinity between the original chitins and the resulting chitosan. Process P4 exhibited the most significant crystallinity difference, around 25.68 %. This change can influence various physicochemical and functional properties of chitosan, including its solubility and viscosity [12]. In the CHS P1 spectrum, the presence of a peak around  $22.8^\circ$ , characteristic of chitin and corresponding to the (120) plane, suggests an incomplete transformation of chitin into chitosan. Additionally, a peak at  $27^\circ$  is observed in CHS P2, as well as in the CHS P3 spectra, with another peak at  $23.7^\circ$ , indicating impurities that could be attributed to minerals or persistent proteins/pigments in the chitosan [61]. In contrast, only the two characteristic peaks of chitosan are observed in CHS P4, confirming that chitosan P4 is



Fig. 3. Visual comparison of raw material (RM) and chitin extracted through P1 (CHT P1), P2 (CHT P2), P3 (CHT P3), and P4 (CHT P4).

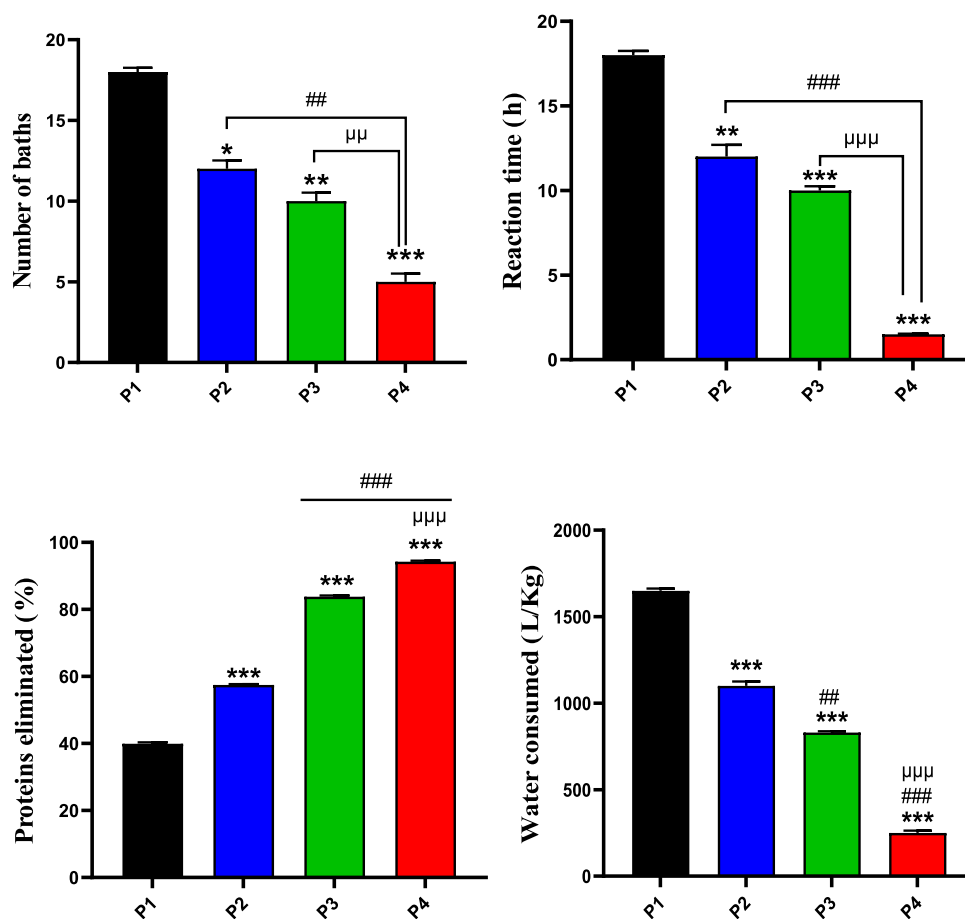
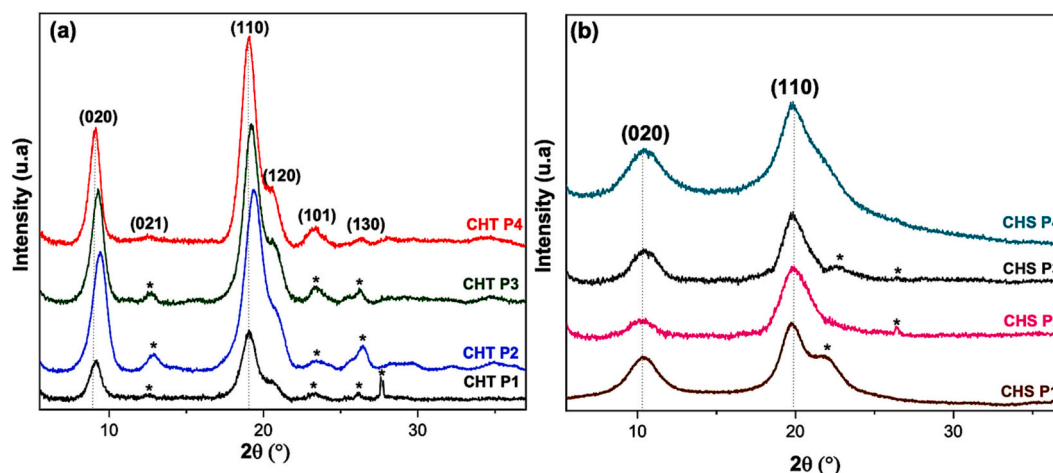


Fig. 4. Histograms showing the Optimized factors during deproteinization step in the different processes (P1, P2, P3 and P4). Values are presented as means ± standard deviation. Statistically significant differences ( $p < 0.05$ ) from the P1 process (Control) are indicated by \* from the P3 process by # and from the P4 process by (μ). Statistical evaluation was performed using a one-way ANOVA ( $p = 0.05$ ).

**Table 5**  
Influence of different extraction processes on yields (%) after each step.

Steps	Delipidation (%)	Demineralization (%)	Deproteinization (%)	Chitin yield (%)	Chitosan yield (%)
Processes					
P1	–	53.50 ± 2.30	19.66 ± 0.58	13.84 ± 1.15	68.57 ± 1.15
P2	87.87 ± 0.62	69.34 ± 5.77 (*)	21.43 ± 0.57 ns	15.43 ± 0.07 ns	72.02 ± 0.57 ns
P3	97.27 ± 0.05 (#)	71.30 ± 0.05 (*)	34.58 ± 0.07 (*/#)	25.72 ± 1.15 (*/#)	74.37 ± 0.66 (*)
P4	97.27 ± 1.15 (#)	71.30 ± 1.15 (*)	41.70 ± 1.15 (*/#/μ)	34.74 ± 1.15 (*/#/μ)	83.33 ± 1.15 (*/#/μ)

Values are presented as means ± standard deviation. Statistically significant differences ( $n = 3$ ;  $p < 0.05$ ) compared with the P1 process (Control) are indicated by \* from the P3 process by # and from the P4 process by (μ). Statistical evaluation was performed using ANOVA with  $p < 0.05$  considered statistically significant between control and treated groups.



**Fig. 5.** XRD spectra of chitins (a) and chitosans (b).

purier than P1, P2, and P3, with the highest crystallinity difference.

Based on the characteristic X-ray peak intensities of chitins and chitosans, the crystallinity indices ( $I_{Cr}$ ) were calculated using Eq. (7). The results in Table 6 show that the  $I_{Cr}$  values of chitin (CHT P1, P2, P3, and P4) are consistently higher than those of chitosan (CHS P1, P2, P3, and P4). These results are consistent with those of [47,62].

Further observation from the results of XRD analysis of chitin revealed a distinct contrast between delipidated chitin (CHT P2, P3 and P4) and non-delipidated chitin (CHT P1). Delipidated chitin exhibited

**Table 6**  
XRD parameters of chitins and chitosans.

	Chitin		Chitosan		$\Delta$ Crystallinity (%)
	$2\theta$ (°)	$I_{Cr}$ (%)	$2\theta$ (°)	$I_{Cr}$ (%)	
P1	9.1	53.3			18.5
	19.06		10.32	34.8	
	23.16		19.72		
	26.6				
P2	9.42	59.49			23.26
	12.9		10.16		
	19.38		19.78	36.23	
	23.44				
	26.2				
P3	9.3	62.23			16.93
	12.6		10.4		
	19.14		19.84	45.3	
	23.28				
	26.44				
P4	9.08	73.38			25.68
	19.06		10.26		
	23.24		19.84	47.7	
	26.02				

well-defined and intense diffraction peaks, indicative of a highly ordered crystal structure. Conversely, non-delipidated chitin (CHT P1) exhibited less intense and less sharp peaks, suggestive of a less ordered crystal structure. These interpretations are similar for chitosan with (CHT P2, P3 and P4) and without any delipidation (CHT P1). These findings reinforce the important role of delipidation by obtaining a more ordered crystalline structure for both chitin and chitosan [63].

The peaks observed in all FTIR spectra (Fig. 6 (a)) of chitins (CHT P1, P2, P3, and P4) included an amide I absorption band at  $1659\text{ cm}^{-1}$ , corresponding to CO—HN intermolecular hydrogen bonds [59], and an amide II band at  $1560\text{ cm}^{-1}$  [64]. Additionally, a broad band was observed at  $3100\text{--}3600\text{ cm}^{-1}$ , corresponding to the stretching of -NH and -OH groups. The peak at  $894\text{ cm}^{-1}$  represents a ring stretching band characteristic of the  $\beta$ -1,4 glycosidic bonds and the absorption peak around  $1050\text{ cm}^{-1}$  is associated with the stretching vibration of the -C-O-C bridge of the glucosamine ring [65]. Peaks at  $3258\text{ cm}^{-1}$  and  $3108\text{ cm}^{-1}$  correspond to the axial deformation of the NH group involved in intermolecular hydrogen bonds. The band observed at  $1315\text{ cm}^{-1}$  indicates CO-NH deformation and the  $\text{CH}_2$  grouping. These results are therefore consistent with those of [12,47,65]. Furthermore, the amide I band at  $1659\text{ cm}^{-1}$  is distinctly split in the FTIR spectra, indicative of a doublet that results from differential hydrogen bonding. This splitting is a defining feature of  $\alpha$ -chitin [66], thereby confirming the  $\alpha$ -chitin structure in all isolated samples.

After the deacetylation of chitins, a significant change in the intensity of the bands was observed, along with the disappearance of some bands (Fig. 6(b)). Specifically, the band observed at  $3108\text{ cm}^{-1}$  disappeared. Additionally, the intensities of the bands at  $1642\text{ cm}^{-1}$  and at  $1560\text{ cm}^{-1}$  observed in the chitin spectra, decreased after deacetylation. These bands are indicative of chitosan [67,68]. The degree of

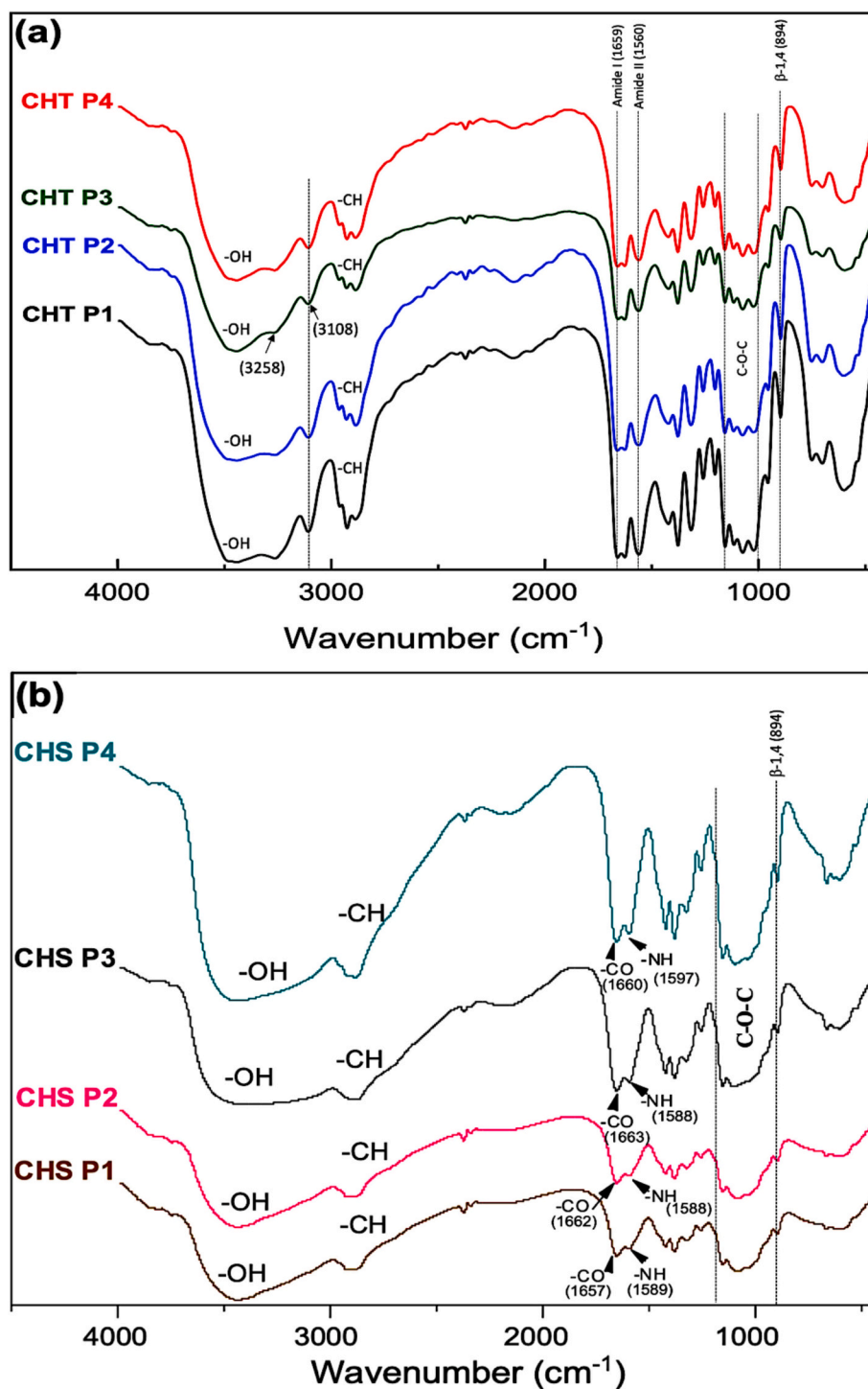


Fig. 6. FTIR spectra of chitins (a) and chitosans (b).

acetylation (DA) of chitosans P1, P2, P3 and P4 was calculated using the Eq. (5) to be  $9.09 \pm 0.18$  %,  $6.33 \pm 0.05$  %,  $6.35 \pm 0.78$  % and  $5.80 \pm 0.07$  % respectively.

<sup>1</sup>H NMR is considered to be the best and most accurate method currently available for calculating the degree of acetylation (DA) [69]. Fig. 7 shows the <sup>1</sup>H NMR spectra of chitosans (CHS P1, P2, P3 and P4). A peak at 4.55 is assigned to the amine proton (H-1-D) with an integration value of 1.00 [62]. Additionally, protons at positions 1 to 6 in the molecule (H-1/6) are observed between 1.5 and 4 ppm [53]. The H-2 of the *N*-deacetylated units (H-2-D) appears at 1.08 ppm [69]. The acetyl proton peak (CH<sub>3</sub>) is more intense in CHS P1 comparing to CHS P4, with

integration values of 0.16 for CHS P1, 0.15 for CHS P2, 0.12 for CHS P3 and 0.09 for CHS P4. The peak at 4.1 ppm is attributed to the solvent used. The DA of chitosans CHS P1, P2, P3 and P4 was calculated to be  $5.04 \pm 0.02$  %,  $4.77 \pm 0.20$  %,  $3.85 \pm 0.14$  % and  $2.92 \pm 0.08$  % respectively. These results are in line with those calculated using FTIR method.

The titration curves obtained from the recovered chitosan (CHS P1, P2, P3 and P4) (Fig. 8) show a clear difference between the two inflection points, which corresponds to the amount of acid consumed for the neutralization of the amine groups within the chitosan molecules [46]. The DA were calculated according to the Eq. (8) (Fig. 9).

Fig. 9 presents the DA determined for the different types of chitosan

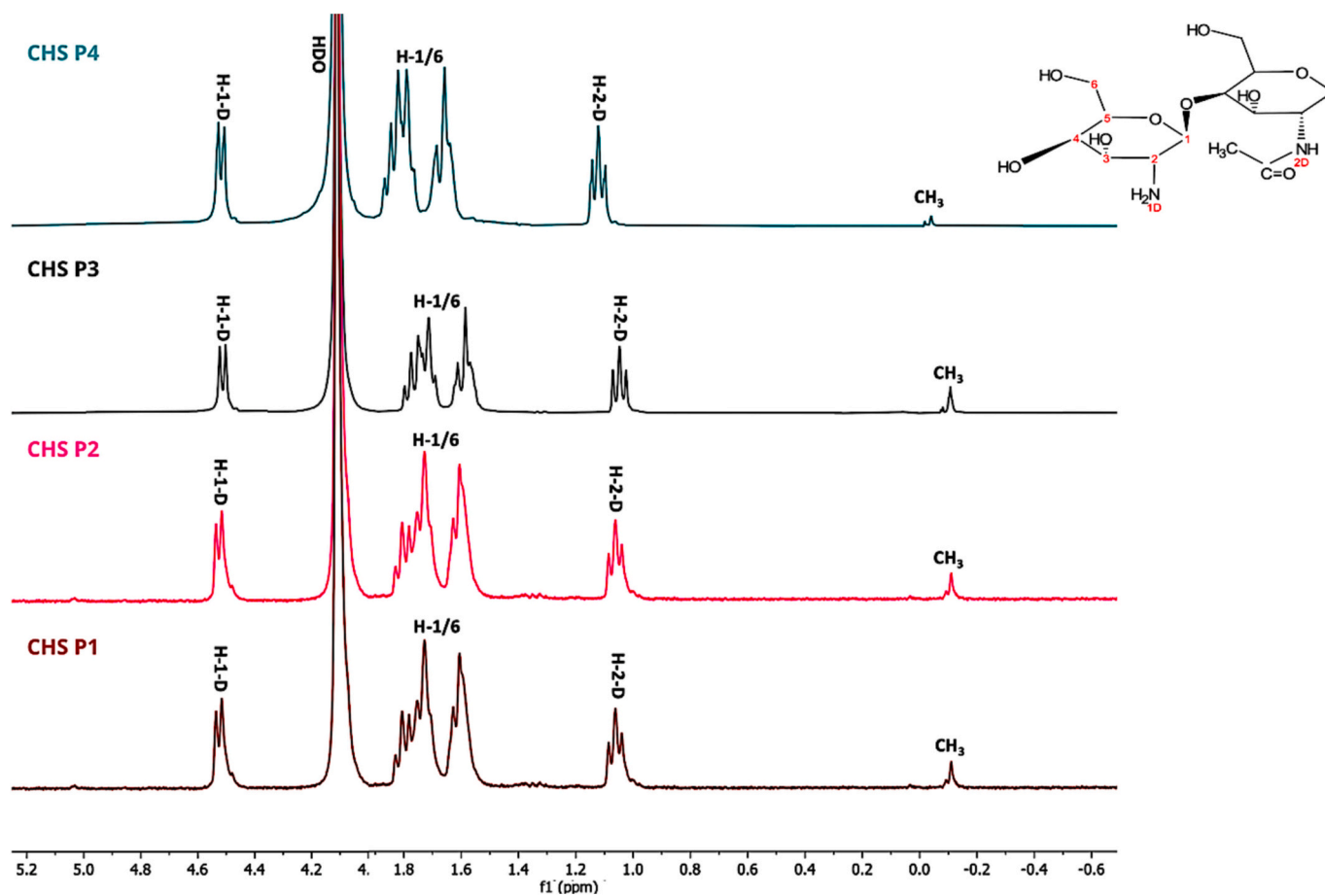


Fig. 7. <sup>1</sup>H NMR spectra (400 MHz, 2 % DCl, 70 °C) of *H. illucens* chitosans (CHS) extracted by P1, P2, P3 and P4.

(CHS P1, CHS P2, CHS P3 and CHS P4). These results are in consistent with the literature for the same categories of beetle species [70,71]. The DA values obtained by the three methods show slight differences, which could be attributed to the precision, accuracy, and reliability of each method [47]. However, the trend of these values is coherent, and the results indicate that CHS P4 is the most deacetylated compared to CHS P1, P2, and P3. This property could be advantageous for environmental applications, such as heavy metal removal and as a plant fortifier [72,73], due to the presence of free amine groups that can rapidly exchange with metals and be protonated to facilitate solubilization.

From the SEM images (Fig. 10), a contrast emerged between the delipidated chitin (CHT P2, P3 and P4) and non-delipidated chitin (CHT P1). Delipidated chitin shows a smoother surface and more regular organization. The lipids associated to chitin form an irregular and granular layer, which gives a rough appearance to the surface observed in SEM. Removal of these lipids reveals a chitin with a more uniform and regular surface, highlighting the high structural purity of the chitinous matrix. Additionally, delipidated chitins (CHT P2, P3 and P4) revealed fine details such as pores and ridges present on the surface contributing to a more homogeneous structure and smoother appearance [63].

The SEM images of chitosan (P1, P2, P3 and P4) show relatively uniform structures with heterogeneous surface presenting disorganized microfibrils, consequently reflecting a reduction in the crystallinity index (Table 6). Additionally, the presence of lighter pores was notable on the surface, particularly evident in for chitosan from process P2 and P3 (Fig. 11).

After plotting the curves of reduced viscosity as a function of the concentration of chitosan solution (P1, P2, P3 and P4), it was possible to deduce the value of the viscometric molar mass of each chitosan by applying the previous equation. Upon the obtained results, a noteworthy

trend emerges: the viscometric molar mass of chitosan varies according to the production processes and can be categorized in the following order:

$$M_v \text{ CHS P4} > M_v \text{ CHS P1} > M_v \text{ CHS P3} > M_v \text{ CHS P2}$$

Process 2 led to a high degradation of chitosan P2 compared to other processes, resulting in a lower viscometric molar mass of 95,316 g.mol<sup>-1</sup> (Fig. 12). This degradation can be attributed to the use of hexane during the delipidation step. The interactions between apolar hexane and polar groups of chitosan disrupt its chemical structure [74]. This results in the breakdown of chemical bonds within the polymer, thereby weakening its strength and mechanical properties. This renders the biopolymer brittle and susceptible to deformation.

Conversely, the chitosan P4 was obtained by the autoclave process, as evidenced by the higher viscometric molar mass of 220,378 g.mol<sup>-1</sup> (Fig. 12). This can be attributed to the shorter duration of the deacetylation step (1 h), this molar mass is considered a good quality for commercial use from shrimp, as it falls within the typical molecular weight range for commercial chitosan products [75,76].

Thermal stability, a critical property in assessing the potential applications of chitin and chitosan, can be evaluated through TGA techniques. Focusing on the thermal degradation of the backbone of chitin and chitosan, Fig. 13 displays a mass loss after water removes, i.e. after 150 °C. The thermal degradation is largely affected by the crystallinity, morphology and molecular weight [77]. Then, the TGA results could not be used alone for chitin configuration determination without the combined use of multiple instrumental analyses, i.e. FTIR, <sup>1</sup>H NMR, XRD and SEM [78]. The thermal degradation of chitins occurs between 280 °C and 450 °C, primarily attributed to the degradation of the chitin chain [79]. The DTG<sub>max</sub> values for chitins are shown in Table 7. CHT P1, P2, P3

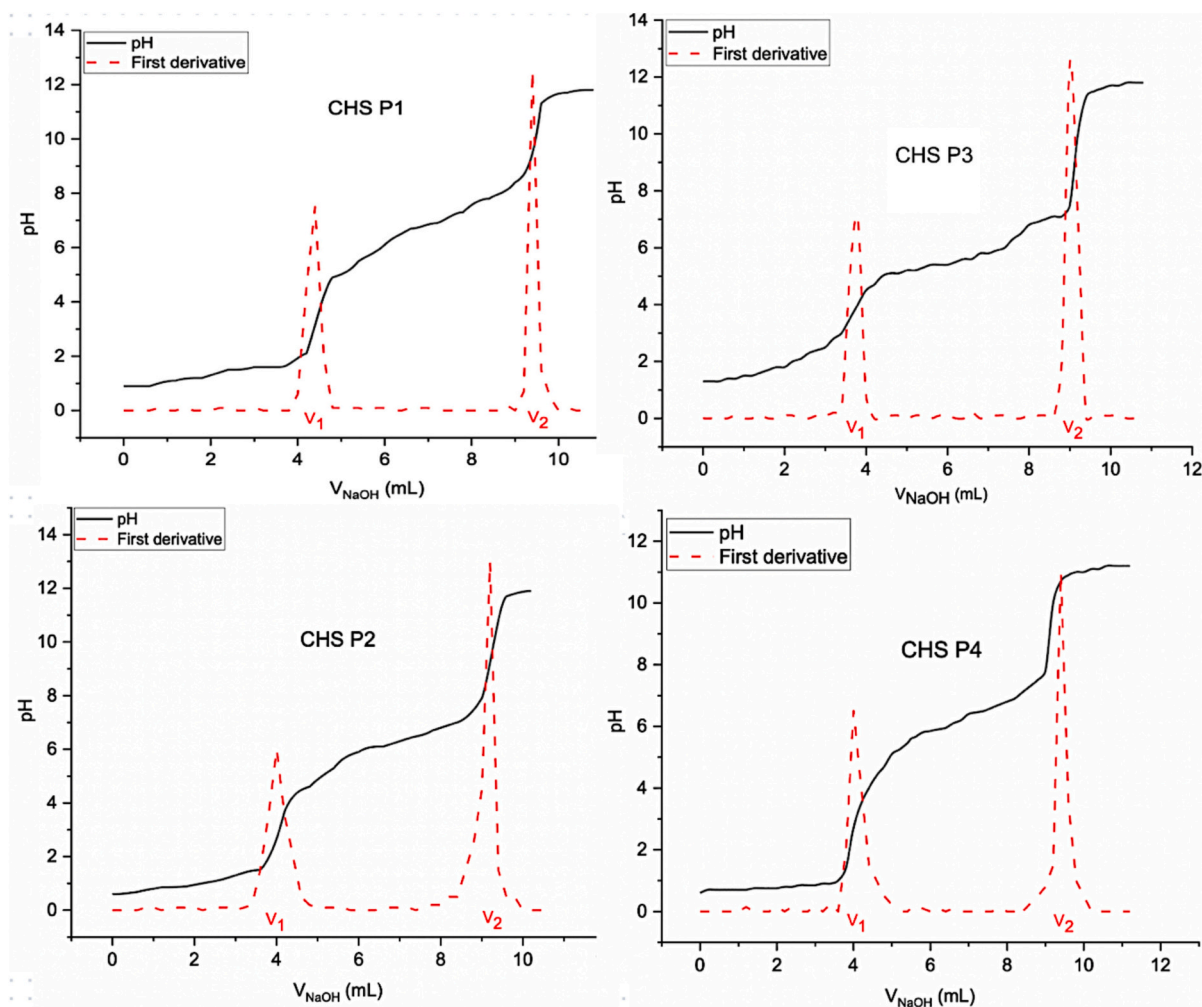


Fig. 8. Potentiometry curves of chitosans P1, P2, P3 and P4.

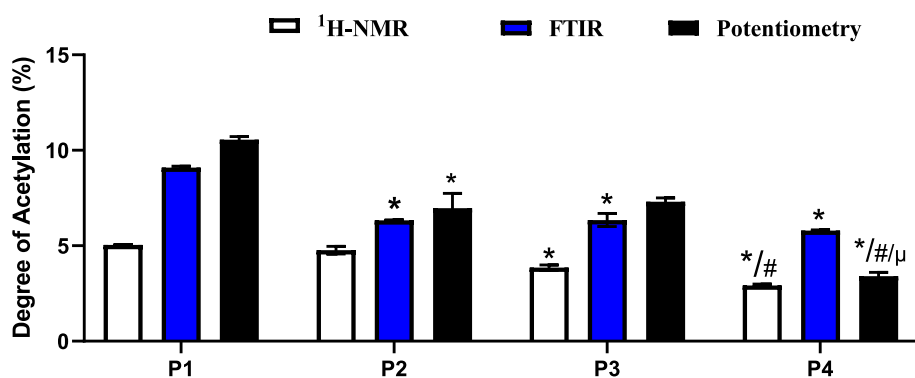


Fig. 9. Histograms showing the comparison of degree of acetylation (DA) values according to three methods: FTIR, <sup>1</sup>H NMR, and Potentiometry. Values are expressed as means  $\pm$  standard deviation. Statistically significant differences ( $n = 5$ ;  $p < 0.05$ ) compared to the P1 process (Control) are indicated by \*, compared to the P3 process by #, and compared to the P4 process by ( $\mu$ ). Statistical evaluation was performed using one-way ANOVA ( $p = 0.05$ ).

and P4 exhibit DTG<sub>max</sub> values of 384 °C, 386 °C, 411 °C and 421 °C, respectively. This confirms the  $\alpha$ -chitin form, which is usually higher than 350 °C [80]. The around 40 °C shift of DTG<sub>max</sub> between P1-P2 and P4, with the same onset behavior, can indirectly, be attributed to a possible higher molecular weight but also to the crystalline structure being more homogeneous and the crystallinity rate (Fig. 5 and Table 6) obtained with P4 process. The TGA curves of different chitosan (CHS P1, P2, P3 and P4) (Fig. 13) display a mass loss between 290 °C and 450 °C,

and it can be attributed to the decomposition of chitosan, especially the acetylated and deacetylated units [81].

Furthermore, the maximum degradation temperatures (DTG<sub>max</sub>) are observed at peaks of 323 °C, 338 °C, 343 °C, and 345 °C, corresponding to CHS P1, CHS P2, CHS P3, and CHS P4, respectively (Table 7). This variation in DTG<sub>max</sub> among the four chitosans can be attributed to the distinct degrees of deacetylation associated with each process, the number of hydrogen bonds, and the influence of crystallinity on their

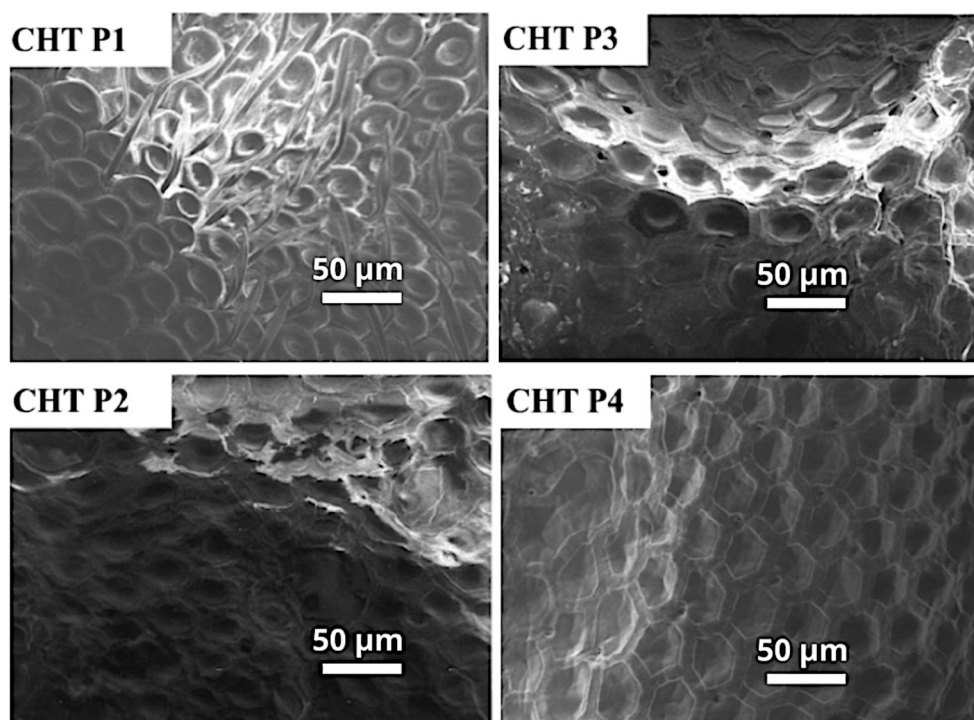


Fig. 10. SEM images of chitins P1, P2, P3 and P4.

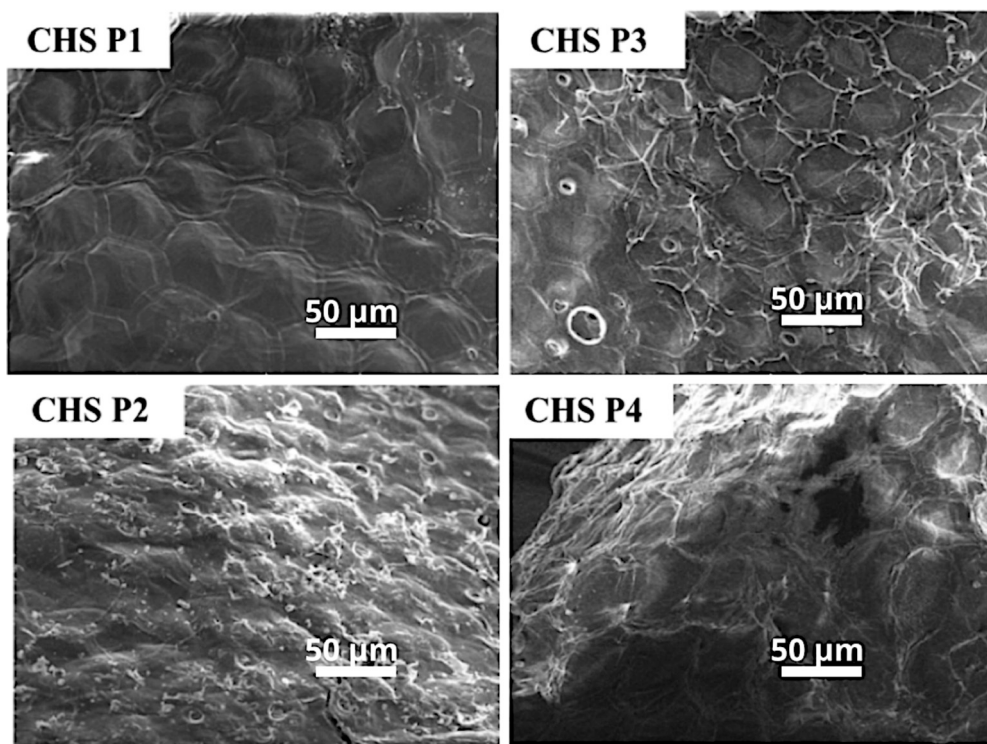


Fig. 11. SEM images of chitosans P1, P2, P3 and P4.

thermal stability [82]. The results suggest that chitin CHT P4 and chitosan CHS P4 possess the highest thermal stability and longer chain lengths compared to the other three chitins and chitosans, as well as compared to chitins obtained through green preparation methods reported in the literature [83].

### 3.3. Influence of the process and role of deacetylation

Optimizing chitin and chitosan extraction from *Hermetia illucens* breeding waste offers a unique opportunity to enhance waste valorization through sustainable and efficient processing. In insect waste valorization, the primary objective is to achieve high-purity chitin with structural integrity that closely resembles its native form, while also

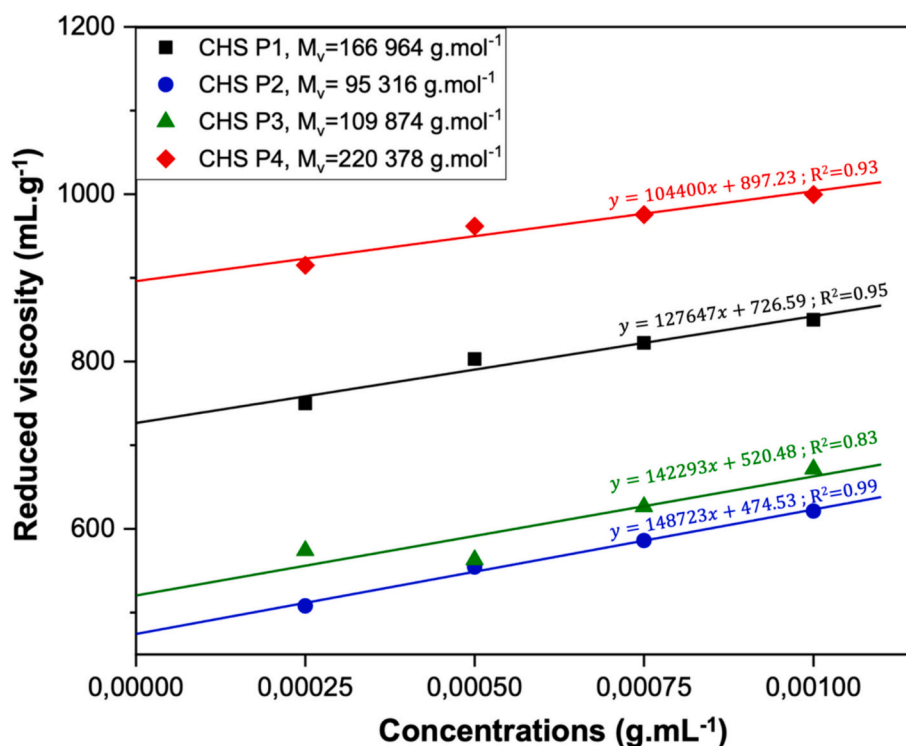


Fig. 12. Examples of the viscosity curves of the chitosan samples CHS P1, P2, P3 and P4 prepared from pupal cases of BSF.

enabling efficient *N*-deacetylation to produce chitosan with desirable properties. Process 4 (P4), optimized in this study, demonstrates significant advantages in purity, yield, and efficiency, making it a promising candidate for industrial applications. This aligns with the fundamental requirements for sustainability and industrial scalability in chitin extraction processes, which rely heavily on maximizing yield, minimizing processing time, and ensuring operational simplicity.

This process allows the production of chitosan that is almost fully deacetylated with a high molecular weight, providing several options for environmental applications. The involvement of an autoclave-assisted process represents an environmentally friendly approach, minimizing processing time while achieving desirable physicochemical properties. When comparing chitin yields from BSF pupal cases across various studies (Table 8), Process 4 stands out with a yield of  $34.74 \pm 1.15\%$ , which is significantly higher than those reported in other studies employing different extraction methods [10]. For instance, chemical methods have reported yields of 14.1 %, 10.7 %, and 9 %, indicating a marked inefficiency compared to P4. Additionally, the microwave assisted process reported by Elouali et al., considered as an ecofriendly method for chitin extraction, yields a lower amount of chitin from prepupal cases of BSF compared to the optimized process P4, which achieves around 21.14 % [84]. Although continuous fermentation technique, recognized as a biological method for chitin extraction, has yielded up to 59.9 % [26], they often require longer processing times and more complex operational requirements, making them less practical for industrial production. In the study by Lin et al., microbial fermentation was applied to BSF pupal waste using *Bacillus licheniformis* A6, achieving a chitin yield of 12.4 % after 10 days of fermentation [85]. While this method leverages a biological approach, its extended duration and lower efficiency highlight the trade-off in yield and operational complexity. Additionally, it is important to note that the described biological approaches [26,85] are limited to the extraction of chitin. For subsequent deacetylation to produce chitosan, chemical methods remain indispensable. Specifically, the chemical protocols employed in related studies utilized 30 % NaOH for 3 h at a ratio of 1:50 [26] and 50 % NaOH for 4 h at the same ratio [85]. Moreover, the microbial method

used in this study retained 7.51 % protein content in the chitin, suggesting lower purity. In contrast, P4 achieved a deproteinization efficiency of  $94.25 \pm 0.6\%$  within a markedly shorter duration ( $1.15 \pm 0.08$  h), reinforcing its suitability for practical and scalable applications with minimal resource expenditure.

Regarding chitosan yields, Process 4 achieves a yield of  $83.33 \pm 1.15\%$ . This is notably higher than the yields obtained through chemical methods, with Elkadaoui et al. reporting only 74 % from BSF pupal cases [32] and Hamdan et al. reporting 75.36 % from *Akis granulifera* [47]. These results highlight the advantages of the autoclave technique, which combines the use of potassium hydroxide, ethanol and mono-ethylene glycol mixture under a pressure of 2.2 bar at 121 °C in a total time of 1 h. This approach facilitates obtaining the highest yield of chitosan by effectively removing proteins and acetyl groups without causing any degradation or yield loss of the chitosan.

In terms of physicochemical properties, the chitin obtained by process 4 shows the highest crystallinity and thermal degradation compared to the other three processes conducted in this study. This indicates that these properties are also advantageous compared to studies that reported extraction from the same source, where the DTG<sub>max</sub> did not exceed 373 °C, and crystallinity did not surpass 69 % (Table 8). This confirms the successful extraction of chitin, which is close to its native form, primarily existing as a semi-crystalline polymer [87]. After *N*-deacetylation, the crystallinity and thermal stability of chitin decreased to 47.7 % and 345 °C, respectively, confirming its successful transformation into chitosan, which inherently has lower crystallinity and thermal stability due to the loss of acetyl groups and increased disorder in the polymer chains [88].

#### 4. Conclusion

Four extraction processes were developed to standardize and determine the best method for extracting chitin and producing chitosan from *Hermetia illucens* breeding waste (pupal cases). Among the processes studied, process P4 showed the highest efficiency in terms of polysaccharide purification, with a yield of 34.74 % for chitin and 83.33 %

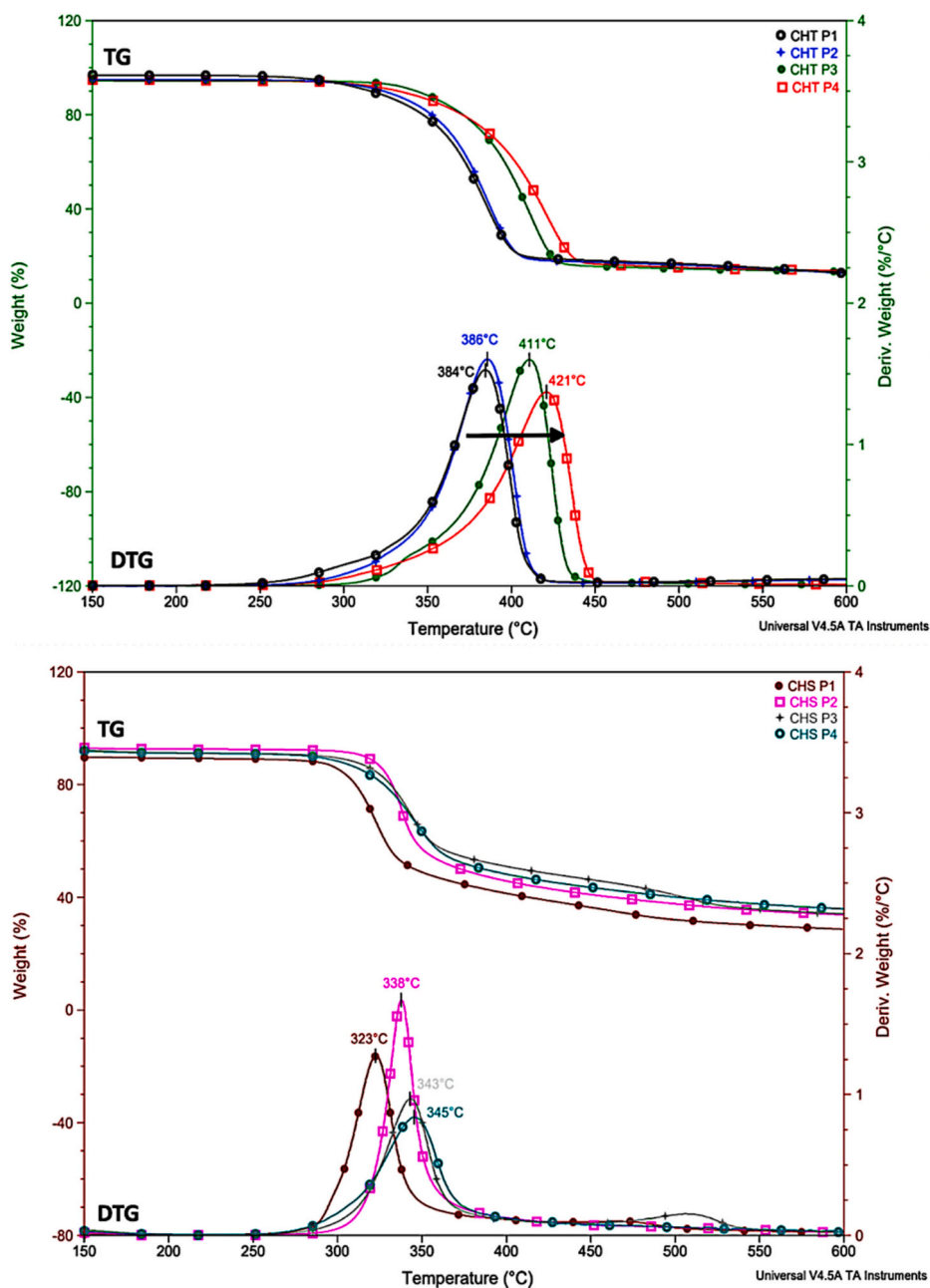


Fig. 13. Thermograms (TG) and their derivatives (DTG) of chitins (CHT) and chitosans (CHS) P1, P2, P3 and P4.

Table 7

DTG<sub>max</sub> of chitins and chitosans from P1, P2, P3 and P4 processes.

	DTG <sub>max</sub> (°C)	
	Chitin	Chitosan
P1	384	323
P2	386	338
P3	411	343
P4	421	345

for chitosan, outperforming the other processes. This process also stands out for its environmentally friendly approach, reducing water use by 80 %, chemical consumption by 83 %, and reaction time by 95 % during the deacetylation step. Additionally, the physicochemical and thermal properties of the chitosan obtained through this process are significantly better than those from the other methods, with a degree of acetylation

(DA) of 2.92 %, crystallinity of 47.7 %, a molecular weight of 220,378 g. mol<sup>-1</sup>, and a DTG<sub>max</sub> of 345 °C. A distinguishing aspect of this process is the incorporation of an autoclave technology, combined with a delipidation step, which preserves the structure and quality of the polysaccharides, unlike the other methods. Therefore, it is more suitable and recommended for extracting polysaccharides from insect waste. However, while this process has proven the most efficient, further developments are necessary. Scale-up studies are needed to fine-tune extraction parameters, ensuring the production of chitosans with physicochemical properties tailored for specific applications using diverse insect biomass types.

#### CRediT authorship contribution statement

**Samia Elouali:** Writing – original draft, Software, Methodology, Investigation, Data curation, Conceptualization. **Youssef Ait Hamdan:** Writing – original draft, Software, Methodology, Data curation,

**Table. 8**

Comparison of chitin and chitosan properties obtained by Process 4 and other extraction methods across different sources.

Study	Extraction method	Source	Yields (%)		DA (%)	Mv (kDa)	I <sub>Cr</sub> (%)		DTG <sub>max</sub> (°)	
			Chitin	Chitosan			Chitin	Chitosan	Chitin	Chitosan
This work	Process 4		34.74 ± 1.15	83.33 ± 1.15	2.92	220.38	73.38	47.7	421	345
[10]	Chemical		14.1	–	–	–	68.44	–	371	–
[63]	Chemical		9	–	–	–	25.20	–	371	–
[86]	Chemical		10.7	–	–	–	64	–	365	–
[26]	Biological	Pupal cases of BSF	59.9	–	18.52	–	68.44	–	373	–
[85]	Biological		12.4	–	–	–	52.8	55.4	–	–
[32]	Chemical		43 ± 1.1	74	4	115	69	–	336	–
[62]	Chemical		17.97	–	3.15	62.24	47.11	30	328	307
[84]	Microwave-assisted process	Prepupal cases of BSF	21.14	65.89	4.1	155	–	51.26	–	326
[12]	Chemical	<i>Periplaneta americana</i> L.	–	–	15.3	75.05	55.08	40.28	–	–
[47]	Chemical	Akis granulifera	24.59 ± 0.39	75.36 ± 1.75	5.48	178	59.8	49	330	320

Conceptualization. **Samira Benali:** Writing – review & editing, Writing – original draft, Investigation, Conceptualization. **Patrick Lhomme:** Writing – review & editing, Writing – original draft. **Matthias Gosselin:** Writing – review & editing, Writing – original draft. **Jean-Marie Raquez:** Writing – original draft, Visualization, Validation, Supervision. **Mohammed Rhazi:** Writing – review & editing, Visualization, Validation, Supervision, Methodology, Conceptualization.

#### Declaration of competing interest

The authors declare that they have no known competing financial interests or personal relationships that could have appeared to influence the work reported in this paper.

#### Acknowledgments

This work is supported by “Académie de Recherche et d’Enseignement supérieur, (ARES)” in the framework of Research & Development Project (2022-2027 Program) between Belgium and Moroccan universities. Dr. Samira Benali acknowledges the European Regional Development Fund (ERDF-FEDER) for general support in the frame of UP\_PLASTICS portofolio. Jean-Marie Raquez is a F.R.S.-FNRS Research Director. We extend our gratitude to the startup EntomoNutris for providing the pupal cases samples of the BSF, which were crucial for conducting this study. We sincerely thank Mr. Hassan Lamtai, laboratory technician at the Department of Biology, Higher Normal School, Cadi Ayyad University for his exceptional support and technical expertise.

#### Data availability

No data was used for the research described in the article.

#### References

- C. Tang, D. Yang, H. Liao, H. Sun, C. Liu, L. Wei, F. Li, Edible insects as a food source: a review, *Food Prod. Process. Nutr.* 1 (2019) 8, <https://doi.org/10.1186/s43014-019-0008-1>.
- F. Fayuni, B. Hasnan, Y. Feng, T. Sun, K. Parraga, M. Schwarz, M. Zarei, Insects as valuable sources of protein and peptides: production, Functional Properties, and Challenges (2023), <https://doi.org/10.3390/foods12234243>.
- L. Torri, M. Li, C. Mao, X. Li, L. Jiang, W. Zhang, M. Li, H. Liu, Y. Fang, S. Liu, G. Yang, X. Hou, Edible Insects: A New Sustainable Nutritional Resource Worth Promoting (2023), <https://doi.org/10.3390/foods12224073>.
- M. Triunfo, E. Tafi, A. Guarnieri, R. Salvia, C. Scieuzo, T. Hahn, S. Zibek, A. Gagliardini, L. Panariello, M.B. Coltelli, A. De Bonis, P. Falabella, Characterization of chitin and chitosan derived from *Hermetia illucens*, a further step in a circular economy process, *Sci. Rep.* 12 (2022), <https://doi.org/10.1038/s41598-022-10423-5>.
- A.W. Almutairi, A. Abomohra, M. Elsayed, A closed-loop approach for enhanced biodiesel recovery from rapeseed biodiesel-based byproducts through integrated glycerol recycling by black soldier fly larvae, *J. Clean. Prod.* 409 (2023) 137236, <https://doi.org/10.1016/j.jclepro.2023.137236>.
- M. Elsayed, J. Wang, H. Wang, Z. Zhou, A.I. Osman, A.W. Almutairi, S. Faisal, A. Abomohra, Conversion of protein-rich waste into biodiesel by *Hermetia illucens*: enhanced energy recovery and reduced greenhouse gas emissions, *Sustain Energy Technol Assess* 66 (2024) 103825, <https://doi.org/10.1016/j.seta.2024.103825>.
- M. Kozma, B. Acharya, R. Bissessur, Chitin, chitosan, and Nanochitin: extraction, synthesis, and applications, *Polymers (Basel)* 14 (2022) 3989, <https://doi.org/10.3390/polym14193989>.
- Y. Ait Hamdan, A. Ait Baba, H. Azraida, H. Kabby, H. Oudadesse, A. Chait, M. Rhazi, In vivo evaluation by oral administration of chitosan combined with bioactive glass against cadmium-induced toxicity in rats, *Int. J. Biol. Macromol.* 276 (2024) 133845, <https://doi.org/10.1016/j.IJBIOMAC.2024.133845>.
- F. El Amerany, M. Rhazi, S. Wahbi, M. Taourirte, A. Meddich, The effect of chitosan, arbuscular mycorrhizal fungi, and compost applied individually or in combination on growth, nutrient uptake, and stem anatomy of tomato, *Sci. Hortic.* 261 (2020) 109015, <https://doi.org/10.1016/j.scienta.2019.109015>.
- H. Wang, K. ur Rehman, W. Feng, D. Yang, R. ur Rehman, M. Cai, J. Zhang, Z. Yu, L. Zheng, Physicochemical structure of chitin in the developing stages of black soldier fly, *Int. J. Biol. Macromol.* 149 (2020) 901–907, doi:<https://doi.org/10.1016/J.IJBIOMAC.2020.01.293>.
- H. Faizan Muneer, A. Nadeem, W. Zaheer Arif, Bioplastics from biopolymers: an eco-friendly and sustainable solution of plastic pollution, *polymer science, Series C* 63 (2021) 47–63, <https://doi.org/10.1134/S1811238221010057>.
- S. Elouali, H. Ait Ali Ouydir, Y. Ait Hamdan, N. Eladlani, M. Rhazi, Chitosan from *Periplaneta americana* L.: a sustainable solution for heavy metals removal, *EuroMediterr J Environ Integr* (2024). doi:<https://doi.org/10.1007/s41207-024-00645-6>.
- H. Nasiri, H. Baghban, R. Teimuri-Mofrad, A. Mokhtarzadeh, Graphitic carbon nitride/magnetic chitosan composite for rapid electrochemical detection of lactose, *Int. Dairy J.* 136 (2023) 105489, <https://doi.org/10.1016/j.idairyj.2022.105489>.
- H. Nasiri, H. Baghban, R. Teimuri-Mofrad, A. Mokhtarzadeh, Chitosan/polyaniline/graphene oxide-ferrocene thin film and highly-sensitive surface plasmon sensor for glucose detection, *Opt. Quant. Electron.* 55 (2023) 948, <https://doi.org/10.1007/s11082-023-05203-y>.
- H. Nasiri, K. Abbasian, H. Baghban, Highly sensitive quantification of amlodipine in real samples using graphene oxide-chitosan surface plasmon resonance sensor, *Sens Actuators A Phys* 368 (2024) 115152, <https://doi.org/10.1016/j.sna.2024.115152>.
- H. Nasiri, K. Abbasian, M. Salahandish, S.N. Elyasi, Sensitive surface plasmon resonance biosensor by optimized carboxylate functionalized carbon nanotubes/chitosan for amlodipine detecting, *Talanta* 276 (2024) 126249, <https://doi.org/10.1016/j.talanta.2024.126249>.
- L. Saghatforoush, T. Mahmoudi, Z. Khorablou, H. Nasiri, A. Bakhtiari, S.A. A. Sajadi, Electro-oxidation sensing of sumatriptan in aqueous solutions and human blood serum by Zn(II)-MOF modified electrochemical delaminated pencil graphite electrode, *Sci. Rep.* 13 (2023) 16803, <https://doi.org/10.1038/s41598-023-44034-5>.
- H. Nasiri, K. Abbasian, H. Baghban, Sensing of lactose by graphitic carbon nitride/magnetic chitosan composites with surface plasmon resonance method, *Food Biosci.* 61 (2024) 104718, <https://doi.org/10.1016/j.fbio.2024.104718>.
- H. Nasiri, K. Abbasian, High-sensitive surface plasmon resonance sensor for melamine detection in dairy products based on graphene oxide /chitosan nanocomposite, *Food Control* 166 (2024) 110761, <https://doi.org/10.1016/j.foodcont.2024.110761>.
- M. Salahandish, R. Ghahramani Bigbaghlou, H. Nasiri, A. Pourziad, Enhanced plasmonic absorption using MIM ring resonator structures for optical detector applications, *Phys. Scr.* 99 (2024) 085552, <https://doi.org/10.1088/1402-4896/ad6497>.
- Global Chitosan Market by Product (Food Grade, Industrial Grade, Pharmaceutical Grade), Source (Crab, Krill, Shrimp), Packaging Material, Application - Forecast 2024-2030, (n.d.). <https://www.researchandmarkets.com/report/chitosan#rel-a0-338576> (accessed May 1, 2024).
- B.T. Iber, N.A. Kasan, D. Torsabo, J.W. Omuwa, A review of various sources of chitin and chitosan in nature, *J Renew Mater* 10 (2022) 1097–1123, <https://doi.org/10.32604/JRM.2022.018142>.
- K. ur Rehman, C. Hollah, K. Wiesotzki, V. Heinz, K. Aganovic, R. ur Rehman, J.-I. Petrusan, L. Zheng, J. Zhang, S. Sohail, M.K. Mansoor, C.I. Rumbos, C. Athanassiou, M. Cai, Insect-derived chitin and chitosan: A still unexploited

- resource for the edible insect sector, Sustainability 15 (2023) 4864. doi:<https://doi.org/10.3390/su15064864>.
- [24] K. Morgan, C. Conway, S. Faherty, C. Quigley, A comparative analysis of conventional and deep eutectic solvent (DES)-mediated strategies for the extraction of chitin from marine crustacean shells, Molecules 26 (2021) 7603, <https://doi.org/10.3390/molecules26247603>.
- [25] N.A. Zainol Abidin, F. Kormin, N.A. Zainol Abidin, N.A.F. Mohamed Anuar, M. F. Abu Bakar, The potential of insects as alternative sources of chitin: an overview on the chemical method of extraction from various sources, Int. J. Mol. Sci. 21 (2020) 4978, <https://doi.org/10.3390/ijms21144978>.
- [26] A. Xiong, L. Ruan, K. Ye, Z. Huang, C. Yu, Extraction of chitin from black soldier fly (*Hermetia illucens*) and its Puparium by using biological treatment, Life 13 (2023) 1424, <https://doi.org/10.3390/life13071424>.
- [27] C. Pedrazzani, L. Righi, F. Vescovi, L. Maistrello, A. Caligiani, Black soldier fly as a new chitin source: extraction, purification and molecular/structural characterization, LWT 191 (2024) 115618, <https://doi.org/10.1016/j.lwt.2023.115618>.
- [28] I. Younes, M. Rinaudo, Chitin and chitosan preparation from marine sources, Structure, Properties and Applications, Mar Drugs 13 (2015) 1133–1174, <https://doi.org/10.3390/md13031133>.
- [29] T. Spranghers, M. Ottoboni, C. Klootwijk, A. Ovyin, S. Deboosere, B. De Meulenaer, J. Michiels, M. Eeckhout, P. De Clercq, S. De Smet, Nutritional composition of black soldier fly (*Hermetia illucens*) prepupae reared on different organic waste substrates, J. Sci. Food Agric. 97 (2017) 2594–2600, <https://doi.org/10.1002/jsfa.8081>.
- [30] E. Mirwandhono, M.I.A. Nasution, Yunilas, extraction of chitin and chitosan black soldier fly (*Hermetia illucens*) prepupa phase on characterization and yield, IOP Conf Ser Earth Environ Sci 1114 (2022) 012019, <https://doi.org/10.1088/1755-1315/1114/1/012019>.
- [31] T. Hahn, E. Tafi, N. Von Seggern, P. Falabella, R. Salvia, J. Thomä, · Eva Febel, M. Fijalkowska, E. Schmitt, L. Stegbauer, · Susanne Zibek, Purification of Chitin from Pupal Exuviae of the Black Soldier Fly *Hermetia illucens* of Novelty 13 (2022) (1993–2008), <https://doi.org/10.1007/s12649-021-01645-1>.
- [32] S. Elkadaoui, M. Azzi, J. Desbrières, J. Zim, Y. El Hachimi, A. Tolaimate, Valorization of *Hermetia illucens* breeding rejects by chitins and chitosans production, Influence of processes and life cycle on their physicochemical characteristics, Int J Biol Macromol 266 (2024) 131314, <https://doi.org/10.1016/J.IJBIOMAC.2024.131314>.
- [33] I. Younes, S. Hajji, V. Frachet, M. Rinaudo, K. Jellouli, M. Nasri, Chitin extraction from shrimp shell using enzymatic treatment, Antitumor, antioxidant and antimicrobial activities of chitosan, Int J Biol Macromol 69 (2014) 489–498, <https://doi.org/10.1016/J.IJBIOMAC.2014.06.013>.
- [34] M.K. Lagat, S. Were, F. Ndwigah, V.J. Kembol, C. Kipkoech, C.M., Tanga, microorganisms antimicrobial activity of chemically and biologically treated chitosan prepared from black soldier fly (*Hermetia illucens*), Pupal Shell Waste (2021), <https://doi.org/10.3390/microorganisms9122417>.
- [35] A. Gougbedji, P. Agbohossou, P.A. Lalèyè, F. Francis, R.C. Megido, Inventaire des coproduits agricoles potentiellement utilisables pour la production de pupes de mouche *Hermetia illucens* (L. 1758) pour l'alimentation piscicole au Bénin, Tropicicultura 38 (2020) 1–18, <https://doi.org/10.25518/2295-8010.1587>.
- [36] R. Zhu, X. Zhang, Y. Wang, L. Zhang, C. Wang, F. Hu, C. Ning, G. Chen, Pectin oligosaccharides from hawthorn (*Crataegus pinnatifida* Bunge. Var. major): Molecular characterization and potential antilytic activities, Food Chem 286 (2019) 129–135, doi:<https://doi.org/10.1016/J.FOODCHEM.2019.01.215>.
- [37] X. Liu, X. Chen, H. Wang, Q. Yang, K. ur Rehman, W. Li, M. Cai, Q. Li, L. Mazza, J. Zhang, Z. Yu, L. Zheng, Dynamic changes of nutrient composition throughout the entire life cycle of black soldier fly, (2017), doi:<https://doi.org/10.1371/journal.pone.0182601>.
- [38] V. Bandura, L. Fialkowska, P. Osadchuk, Y. Levtrynaika, A. Palvashova, INVESTIGATION OF PROPERTIES OF SUNFLOWER AND RAPESEED OILS OBTAINED BY THE SOXHLET AND MICROWAVE EXTRACTION METHODS, Agraarteasud 33 (2022) 48–58, <https://doi.org/10.15159/jas.22.17>.
- [39] M.M. Bradford, A rapid and sensitive method for the quantitation of microgram quantities of protein utilizing the principle of protein-dye binding, Anal. Biochem. 72 (1976) 248–254, [https://doi.org/10.1016/0003-2697\(76\)90527-3](https://doi.org/10.1016/0003-2697(76)90527-3).
- [40] M.R. Kasaai, A review of several reported procedures to determine the degree of N-acetylation for chitin and chitosan using infrared spectroscopy, Carbohydr. Polym. 71 (2008) 497–508, <https://doi.org/10.1016/J.CARBPOL.2007.07.009>.
- [41] M.L. Duarte, M.C. Ferreira, M.R. Marvão, J. Rocha, An optimised method to determine the degree of acetylation of chitin and chitosan by FTIR spectroscopy, Int. J. Biol. Macromol. 31 (2002) 1–8, [https://doi.org/10.1016/S0141-8130\(02\)00039-9](https://doi.org/10.1016/S0141-8130(02)00039-9).
- [42] R.H. Chen, M.L. Tsaih, Effect of temperature on the intrinsic viscosity and conformation of chitosans in dilute HCl solution, Int. J. Biol. Macromol. 23 (1998) 135–141, [https://doi.org/10.1016/S0141-8130\(98\)00036-1](https://doi.org/10.1016/S0141-8130(98)00036-1).
- [43] M. Rinaudo, M. Milas, P. Le Dung, Characterization of chitosan, Influence of ionic strength and degree of acetylation on chain expansion, Int J Biol Macromol 15 (1993) 281–285, [https://doi.org/10.1016/0141-8130\(93\)90027-J](https://doi.org/10.1016/0141-8130(93)90027-J).
- [44] R. Rotaru, M. Savin, N. Tudorachi, C. Peptu, P. Samoila, L. Sacarescu, V. Harabagiu, Ferromagnetic iron oxide-cellulose nanocomposites prepared by ultrasonication, Polym. Chem. 9 (2018) 860–868, <https://doi.org/10.1039/c7py01587a>.
- [45] N. Balázs, P. Sipos, Limitations of pH-potentiometric titration for the determination of the degree of deacetylation of chitosan, Carbohydr. Res. 342 (2007) 124–130, <https://doi.org/10.1016/J.CARRES.2006.11.016>.
- [46] A. Tolaimate, J. Desbrières, M. Rhazi, A. Alagui, M. Vincendon, P. Vottero, On the influence of deacetylation process on the physicochemical characteristics of chitosan from squid chitin, Polymer (Guildf) 41 (2000) 2463–2469, [https://doi.org/10.1016/S0032-3861\(99\)00400-0](https://doi.org/10.1016/S0032-3861(99)00400-0).
- [47] Y.A. Hamdan, S. Elouali, N. Eladlani, B. Lefeuvre, H. Oudadesse, M. Rhazi, Investigation on *Akis granulifera* (Coleoptera, Sahlberg, 1823) as a potential source of chitin and chitosan: extraction, characterization and hydrogel formation, Int. J. Biol. Macromol. 252 (2023) 126292, <https://doi.org/10.1016/J.IJBIOMAC.2023.126292>.
- [48] M. Triunfo, E. Tafi, A. Guarnieri, R. Salvia, C. Scieuzo, T. Hahn, S. Zibek, A. Gagliardini, L. Panariello, M.B. Coltelli, A. De Bonis, P. Falabella, Characterization of chitin and chitosan derived from *Hermetia illucens*, a further step in a circular economy process, (123AD), doi:<https://doi.org/10.1038/s41598-022-10423-5>.
- [49] R. Smets, B. Verbinen, I. Van De Voorde, G. Aerts, J. Claes, · Mik, V. Der Borgh, Sequential extraction and characterisation of lipids, proteins, and chitin from black soldier fly (*Hermetia illucens*) Larvae, Prepupae, and Pupae, Waste Biomass Valorization 11 (2020) 6455–6466, doi:<https://doi.org/10.1007/s12649-019-00924-2>.
- [50] I. Artilia, Z.Y. Dewi, W. Shofiani, W.N. Auli, N. Ahmad, Extraction and Characterization of Chitosan from Eco-Green <i>Hermetia illucens</i> for Application in Dentistry, Key Eng. Mater. 965 (2023) 45–50, doi:<https://doi.org/10.4028/p-p8hENm>.
- [51] J.M. Paige, L. Ma, C. Chigbu, al ·, Y. Niu, J. Sunarso, F. Liang, A. Nafisah, R. Mutia, A. Jayanegara, Chemical composition, chitin and cell wall nitrogen content of Black Soldier Fly (*Hermetia illucens*) larvae after physical and biological treatment You may also like An Investigation of the Electrochemical Activity of (Ba/Sr)FeO 3-y Anodes A Comparative Study of Oxygen Reduction Reaction on Bi- and La-Doped SrFeO 3 Perovskite Cathodes Chemical composition, chitin and cell wall nitrogen content of Black Soldier Fly (*Hermetia illucens*) larvae after physical and biological treatment, IOP Conf Ser Mater Sci Eng 546 (2019), doi:<https://doi.org/10.1088/1757-899X/546/4/042028>.
- [52] N.S. Liland, I. Biancarosa, P. Araujo, D. Biemans, C.G. Bruckner, R. Waagbø, B. E. Torstensen, E.-J. Lock, Modulation of Nutrient Composition of Black Soldier Fly (*Hermetia illucens*) Larvae by Feeding Seaweed-Enriched Media, 2017, <https://doi.org/10.1371/journal.pone.0183188>.
- [53] Y. Ait Hamdan, S. Elouali, H. Oudadesse, B. Lefeuvre, M. Rhazi, Exploring the potential of chitosan/aragonite biocomposite derived from cuttlebone waste: elaboration, physicochemical properties and in vitro bioactivity, Int. J. Biol. Macromol. 267 (2024) 131554, <https://doi.org/10.1016/J.IJBIOMAC.2024.131554>.
- [54] A. Caligiani, A. Marseglia, G. Leni, S. Baldassarre, L. Maistrello, A. Dossena, S. Sforza, Composition of black soldier fly prepupae and systematic approaches for extraction and fractionation of proteins, lipids and chitin, Food Res. Int. 105 (2018) 812–820, <https://doi.org/10.1016/J.FOODRES.2017.12.012>.
- [55] C.-Y. Wong, S.-S. Rosli, Y. Uemura, Y.C. Ho, A. Leejeerajumnean, W. Kiatkittipong, C.-K. Cheng, M.-K. Lam, J.-W. Lim, Potential Protein and Biodiesel Sources from Black Soldier Fly Larvae: Insights of Larval Harvesting Instar and Fermented Feeding Medium 12 (2019) 1570, <https://doi.org/10.3390/en12081570>.
- [56] A. Nafary, S.A. Mousavi Nezhad, S. Jalili, Extraction and characterization of chitin and chitosan from *Tenebrio Molitor* beetles and Investigation of its antibacterial effect against *Pseudomonas aeruginosa*, Adv. Biomed. Res. 12 (2023) 96, [https://doi.org/10.4103/abr.abr\\_205\\_22](https://doi.org/10.4103/abr.abr_205_22).
- [57] K. Mohan, T. Muralisankar, R. Jayakumar, C. Rajeev Gandhi, A study on structural comparisons of  $\alpha$ -chitin extracted from marine crustacean shell waste, Carbohydrate Polymer Technologies and Applications 2 (2021) 100037, <https://doi.org/10.1016/j.carpta.2021.100037>.
- [58] M. Jang, B. Kong, Y. Jeong, C.H. Lee, J. Nah, Physicochemical characterization of  $\alpha$ -chitin,  $\beta$ -chitin, and  $\gamma$ -chitin separated from natural resources, J. Polym. Sci. A Polym. Chem. 42 (2004) 3423–3432, <https://doi.org/10.1002/pola.20176>.
- [59] S. Abolghassem, S. Molaei, S. Javanshir, Preparation of  $\alpha$ -chitin-based nanocomposite as an effective biocatalyst for microwave aided domino reaction, Heliyon 5 (2019) e02036, <https://doi.org/10.1016/j.heliyon.2019.e02036>.
- [60] J. Kumirska, M. Czerwicka, Z. Kaczynski, A. Bychowska, K. Brzozowski, J. Thöming, P. Stepnowski, Application of spectroscopic methods for structural analysis of chitin and chitosan, Mar. Drugs 8 (2010) 1567–1636, <https://doi.org/10.3390/md8051567>.
- [61] N.M. Julkapli, Z. Ahmad, H.M. Akil, A.A., Bin Mohamed, X-Ray Diffraction Studies of Cross Linked Chitosan with Different Cross Linking Agents for Waste Water Treatment Application, 2010, pp. 106–111, <https://doi.org/10.1063/1.3295578>.
- [62] S. Elouali, O. Dahbane, Y. Ait Hamdan, N. Eladlani, M. Rhazi, Exploring the potential use of chitosan derived from *Hermetia illucens* waste for olive oil mill wastewater treatment, EuroMediterr J Environ Integr (2024), <https://doi.org/10.1007/s41207-024-00593-1>.
- [63] D. Purkayastha, S. Sarkar, Physicochemical Structure Analysis of Chitin Extracted from Pupa Exuviae and Dead Imago of Wild Black Soldier Fly (*Hermetia illucens*) 28 (2020) 445–457, <https://doi.org/10.1007/s10924-019-01620-x>.
- [64] N.M. Farokhi, J.M. Milani, Z.R. Amiri, Production and comparison of structural, thermal and physical characteristics of chitin nanoparticles obtained by different methods, Sci. Rep. 14 (2024) 14594, <https://doi.org/10.1038/s41598-024-65117-x>.
- [65] Y.A. Hamdan, H. Oudadesse, S. Elouali, N. Eladlani, B. Lefeuvre, M. Rhazi, Exploring the potential of chitosan from royal shrimp waste for elaboration of chitosan/bioglass biocomposite: characterization and “in vitro” bioactivity, Int. J. Biol. Macromol. (2024) 134909, <https://doi.org/10.1016/j.ijbiomac.2024.134909>.

- [66] M. Jang, B. Kong, Y. Jeong, C.H. Lee, J. Nah, Physicochemical characterization of  $\alpha$ -chitin,  $\beta$ -chitin, and  $\gamma$ -chitin separated from natural resources, *J. Polym. Sci. A Polym. Chem.* 42 (2004) 3423–3432, <https://doi.org/10.1002/pola.20176>.
- [67] M. Kaya, T. Baran, M. Asan-Ozusaglam, Y. Selim Cakmak, K. Ozcan Tozak, A. Mol, A. Menten, G. Sezen, Extraction and characterization of chitin and chitosan with antimicrobial and antioxidant activities from cosmopolitan Orthoptera species (Insecta), *Biotechnol. Bioprocess Eng.* 20 (2015) 168–179, <https://doi.org/10.1007/s12257-014-0391-z>.
- [68] Y.M. Chen, S. Pekdemir, I. Bilican, B. Koc-Bilican, B. Cakmak, A. Ali, L.S. Zang, M. S. Onses, M. Kaya, Production of natural chitin film from pupal shell of moth: fabrication of plasmonic surfaces for SERS-based sensing applications, *Carbohydr. Polym.* 262 (2021) 117909, <https://doi.org/10.1016/j.carbpol.2021.117909>.
- [69] C.S. Shin, D.Y. Kim, W.S. Shin, Characterization of chitosan extracted from mealworm beetle (*Tenebrio molitor*, Zophobas morio) and Rhinoceros beetle (*Allomyrina dichotoma*) and their antibacterial activities, *Int. J. Biol. Macromol.* 125 (2019) 72–77, <https://doi.org/10.1016/j.ijbiomac.2018.11.242>.
- [70] T. Marmier, C.R. Szczepanski, C. Candet, A. Zenerino, R.P. Godeau, G. Godeau, Investigation on *Mecynorhina torquata* Drury, 1782 (Coleoptera, Cetoniidae, Goliathini) cuticle: surface properties, chitin and chitosan extraction, *Int. J. Biol. Macromol.* 164 (2020) 1164–1173, <https://doi.org/10.1016/j.ijbiomac.2020.07.155>.
- [71] J. Ma, C. Xin, C. Tan, Preparation, physicochemical and pharmaceutical characterization of chitosan from *Catharsius molossus* residue, *Int. J. Biol. Macromol.* 80 (2015) 547–556, <https://doi.org/10.1016/j.ijbiomac.2015.07.027>.
- [72] A. Gamage, N. Jayasinghe, P. Thiviya, M.L.D. Wasana, O. Merah, T. Madhujith, J. R. Koduru, Recent application prospects of chitosan based composites for the metal contaminated wastewater treatment, *Polymers (Basel)* 15 (2023) 1453, <https://doi.org/10.3390/polym15061453>.
- [73] A. Olohigbe, O. Etiosa, O. Wesley, Highly Deacetylated chitosan as low-cost adsorbent material for removal of heavy metals from water, *Asian Journal of Physical and Chemical Sciences* 5 (2018) 1–7, <https://doi.org/10.9734/AJOPACS/2018/38599>.
- [74] S. Bensalem, B. Hamdi, S. Del Confetto, R. Calvet, Characterization of surface properties of chitosan/bentonite composites beads by inverse gas chromatography, *Int. J. Biol. Macromol.* 166 (2021) 1448–1459, <https://doi.org/10.1016/j.ijbiomac.2020.11.024>.
- [75] F. Parthiban, S. Balasundari, A. Gopalakannan, K. Rathnakumar, S. Felix, Comparison of the quality of chitin and chitosan from shrimp, crab and Squilla waste, current world, *Environment* 12 (2017) 670–677, <https://doi.org/10.12944/CWE.12.3.18>.
- [76] A. Islam, M.S. Islam, M.U.M.A. Zakaria, S.C. Paul, A.A. Mamun, Extraction and worth evaluation of chitosan from shrimp and prawn co-products, *Am. J. Food Technol.* 15 (2019) 43–48, <https://doi.org/10.3923/ajft.2020.43.48>.
- [77] H. Zhu, H. Tang, F. Li, H. Sun, L. Tong, Effect of milling intensity on the properties of chitin, chitosan and chitosan films obtained from grasshopper, *Int. J. Biol. Macromol.* 239 (2023) 124249, <https://doi.org/10.1016/j.ijbiomac.2023.124249>.
- [78] Y. Yu, X. Liu, J. Miao, K. Leng, Chitin from Antarctic krill shell: eco-preparation, detection, and characterization, *Int. J. Biol. Macromol.* 164 (2020) 4125–4137, <https://doi.org/10.1016/j.ijbiomac.2020.08.244>.
- [79] A. Hassainia, H. Satha, S. Boufi, Chitin from *Agaricus bisporus*: extraction and characterization, *Int. J. Biol. Macromol.* 117 (2018) 1334–1342, <https://doi.org/10.1016/j.ijbiomac.2017.11.172>.
- [80] Q. Wu, E. Jungstedt, M. Šoltéssová, N.E. Mushi, L.A. Berglund, High Strength Nanostructured Films Based on Well-Preserved  $\beta$ -Chitin Nanofibrils †, 2019, <https://doi.org/10.1039/c9nr02870f>.
- [81] K. Mohan, A.R. Ganesan, T. Muralisankar, R. Jayakumar, P. Sathishkumar, V. Uthayakumar, R. Chandirasekar, N. Revathi, Recent insights into the extraction, characterization, and bioactivities of chitin and chitosan from insects, *Trends Food Sci. Technol.* 105 (2020) 17–42, <https://doi.org/10.1016/j.tifs.2020.08.016>.
- [82] M. Kaya, M. Asan-Ozusaglam, S. Erdogan, Comparison of antimicrobial activities of newly obtained low molecular weight scorpion chitosan and medium molecular weight commercial chitosan, *J. Biosci. Bioeng.* 121 (2016) 678–684, <https://doi.org/10.1016/j.jbiosc.2015.11.005>.
- [83] T.M. Le, C.L. Tran, T.X. Nguyen, Y.H.P. Duong, P.K. Le, V.T. Tran, Green preparation of chitin and Nanochitin from black soldier Fly for production of biodegradable packaging material, *J. Polym. Environ.* 31 (2023) 3094–3105, <https://doi.org/10.1007/s10924-023-02793-2>.
- [84] S. Elouali, Y. Ait Hamdan, M. Belmajdoub, M. Rhazi, Green chitosan extraction from *Hermetia illucens* breeding waste (prepupal cases): characterization and bioadsorption activity, *Int. J. Biol. Macromol.* 281 (2024) 136449, <https://doi.org/10.1016/j.ijbiomac.2024.136449>.
- [85] Y.-S. Lin, S.-H. Liang, W.-L. Lai, J.-X. Lee, Y.-P. Wang, Y.-T. Liu, S.-H. Wang, M.-H. Lee, Sustainable extraction of chitin from spent pupal Shell of black soldier Fly, *Processes* 9 (2021) 976, <https://doi.org/10.3390/pr9060976>.
- [86] L. Soetemans, M. Uyttbroek, L. Bastiaens, Characteristics of chitin extracted from black soldier fly in different life stages, *Int. J. Biol. Macromol.* 165 (2020) 3206–3214, <https://doi.org/10.1016/j.ijbiomac.2020.11.041>.
- [87] K. Piekarska, M. Sikora, M. Owczarek, J. Jóźwik-Pruska, M. Wiśniewska-Wrona, Chitin and chitosan as polymers of the future—obtaining, modification, life cycle assessment and Main directions of application, *Polymers (Basel)* 15 (2023) 793, <https://doi.org/10.3390/polym15040793>.
- [88] N. Isobe, Y. Kaku, S. Okada, S. Kawada, K. Tanaka, Y. Fujiwara, R. Nakajima, D. Bissessur, C. Chen, Identification of chitin allomorphs in poorly crystalline samples based on the complexation with Ethylenediamine, *Biomacromolecules* 23 (2022) 4220–4229, <https://doi.org/10.1021/acs.biomac.2c00714>.